[redacted]

CENTRAL RESEARCH LIBRARY
DOCUMENT COLLECTION

MARTIN MARIETTA ENERGY SYSTEMS LIBRARIES
3 4456 0360633 7

ORNL-1437
Progress

DECLASSIFIED
CLASSIFICATION CHANGED TO:
BY AUTHORITY OF: AEC - 6-12-62
BY: A. Bowman 8/10/82

LABORATORY RECORDS
1954

METALLURGY DIVISION

QUARTERLY PROGRESS REPORT

FOR PERIOD ENDING OCTOBER 31, 1952

AEC RESEARCH AND DEVELOPMENT REPORT

CENTRAL RESEARCH LIBRARY
DOCUMENT COLLECTION

LIBRARY LOAN COPY

DO NOT TRANSFER TO ANOTHER PERSON

If you wish someone else to see this document, send in name with document and the library will arrange a loan.

OAK RIDGE NATIONAL LABORATORY
OPERATED BY
CARBIDE AND CARBON CHEMICALS COMPANY
A DIVISION OF UNION CARBIDE AND CARBON CORPORATION

UCC

POST OFFICE BOX P
OAK RIDGE, TENNESSEE

[redacted]

[redacted]

ORNL-1437

This document consists of 51 pages.
Copy 5 of 140 copies. Series A.

Contract No. W-7405-eng-26

METALLURGY DIVISION

QUARTERLY PROGRESS REPORT

for Period Ending October 31, 1952

J. H. Frye, Jr., Director

EDITED BY

W. H. Bridges

DATE ISSUED

JAN 28 1953

OAK RIDGE NATIONAL LABORATORY
operated by
CARBIDE AND CARBON CHEMICALS COMPANY
A Division of Union Carbide and Carbon Corporation
Post Office Box P
Oak Ridge, Tennessee

[redacted]

[redacted]

MARTIN MARIETTA ENERGY SYSTEMS LIBRARIES

3 4456 0360633 7

[redacted]

ORNL-1437
Progress

INTERNAL DISTRIBUTION

1. G. T. Felbeck (C&CCC)
2. Biology Library
3. Health Physics Library
4. Metallurgy Library
5-6. Central Research Library
7. Reactor Experimental Engineering Library
8-13. Central Files
14. C. E. Center
15. C. E. Larson
16. W. B. Humes (K-25)
17. L. B. Emlet (Y-12)
18. A. M. Weinberg
19. E. H. Taylor
20. E. J. Murphy
21. E. D. Shipley
22. J. H. Frye, Jr.
23. F. C. VonderLage
24. R. C. Briant
25. J. A. Swartout
26. S. C. Lind
27. F. L. Steahly
28. A. H. Snell
29. A. Hollaender
30. M. T. Kelley
31. K. Z. Morgan
32. J. S. Felton
33. A. S. Householder
34. C. S. Harrill
35. C. E. Winters
36. D. S. Billington
37. D. W. Cardwell
38. E. M. King
39. A. J. Miller
40. D. D. Cowen
41. P. M. Reyling
42. W. H. Bridges
43. G. C. Williams
44. L. K. Jetter
45. E. J. Boyle
46. W. D. Manly
47. C. D. Susano
48. W. W. Parkinson
49. R. J. Gray
50. B. S. Borie
51. D. C. Vreeland
52. E. E. Stansbury
53. G. P. Smith
54. J. E. Cunningham
55. R. S. Crouse
56. R. E. Adams
57. J. H. Erwin
58. J. O. Betterton, Jr.
59. L. D. Dyer
60. G. M. Adamson
61. E. S. Bomar
62. F. H. Eckert
63. T. W. Fulton
64. W. J. Fretague
65. R. B. Oliver
66. J. T. Howe
67. T. H. Blewitt
68. W. E. Taylor
69. J. H. Crawford, Jr.
70. J. C. Wilson
71. [illegible]. W. Savage
72. E. E. Hoffman
73. W. [illegible] Leonard
74. J. A. Milko
75. J. M. Warde
76. E. C. Cruetz (consultant)
77. E. P. Wigner (consultant)
78. W. W. Grigorieff (consultant)

[redacted]

[redacted]

[redacted]

EXTERNAL DISTRIBUTION

79-86. Argonne National Laboratory
87-94. Atomic Energy Commission, Washington
95. Battelle Memorial Institute
96-99. Brookhaven National Laboratory
100-103. Carbide and Carbon Chemicals Company (Y-12)
104-105. Knolls Atomic Power Laboratory
106-107. General Electric Company, Richland
108-110. General Electric Company (ANPP)
111. Hanford Operations Office
112. Idaho Operations Office (Phillips Petroleum Co.)
113-116. Los Alamos
117. Massachusetts Institute of Technology (Kaufmann)
118-119. New York Operations Office
120. Patent Branch, Washington
121. Savannah River Operations Office, Wilmington
122-136. Technical Information Service, Oak Ridge
137-140. University of California Radiation Laboratory

[redacted]

[redacted]

[redacted]

Reports previously issued in this series are as follows

ORNL-28	Period Ending March 1, 1948
ORNL-69	Period Ending May 31, 1948
ORNL-407	Period Ending July 31, 1949
ORNL-511	Period Ending October 31, 1949
ORNL-583	Period Ending January 31, 1950
ORNL-754	Period Ending April 30, 1950
ORNL-827	Period Ending July 31, 1950
ORNL-910	Period Ending October 31, 1950
ORNL-987	Period Ending January 31, 1951
ORNL-1033	Period Ending April 30, 1951
ORNL-1108	Period Ending July 31, 1951
ORNL-1161	Period Ending October 31, 1951
ORNL-1267	Period Ending January 31, 1952
ORNL-1302	Period Ending April 30, 1952
ORNL-1366	Period Ending July 31, 1952

[redacted]

[redacted]

[redacted]

CONTENTS

	Page
SUMMARY	1
PHYSICAL METALLURGY OF REACTOR MATERIALS	3
Alloy Development	3
Physical Properties of Thorium	4
Recrystallization	5
ANP PROGRAM	7
Welding and Brazing	7
Fabrication	10
Mechanical Testing	17
Dynamic Corrosion	18
Static Corrosion	25
Physical Chemistry of Corrosion	28
CERAMICS RESEARCH	38
Ceramics Coatings for Metals	38
Cermet Investigation	38
Hafnium Carbide Investigation	38
ANP Reactor Design – Ceramic Reflector	39
Slurry for Magnesia Crucibles	40
High-Temperature X-Ray Studies of Thorium and Hafnium Oxide	40
HRP METALLURGY	40
Welding and Fabrication Specifications for Stainless Steel and Pressure Vessel Steels	40
Surface Hardening of Titanium for Valve Trim	40
Titanium Parts for Pumps	41
Cooperation with HRP Corrosion Group	41
Physical Metallurgy of Titanium	41
FABRICATION RESEARCH	42
Production of MTR Fuel and Control Rod Elements	42
MTR Fabrication Studies	42
Fabrication of Replacement Elements for LITR	44
Miscellaneous Fabrication Work	44
Uranium Fuel Plate Program for Du Pont	45

[redacted]

[redacted]

METALLURGY DIVISION QUARTERLY PROGRESS REPORT

SUMMARY

PHYSICAL METALLURGY OF REACTOR MATERIALS

In the study of thorium alloys, it has been found that the addition of columbium and vanadium to Ames thorium produces a slight strengthening effect with the first small additions but that large additions result in a lowering of strength with corresponding increases in ductility.

The melting point of iodide thorium has been measured as being 1755°C. The curve of electrical resistivity vs. temperature for this material shows an anomalous sharp increase at 1350°C. Expansion curves do not show this discontinuity. X-ray diffraction measurements indicate a possible allotropic transformation in thorium in the temperature range of the abrupt increase in electrical resistivity. More exact measurements are being made.

Studies of a series of thorium-carbon alloys, with carbon content up to 0.13%, indicate that carbon does not affect the temperatures for the start and completion of recrystallization.

ANP PROGRAM

Welding specifications have been prepared for the joining of Inconel pipe and fittings for use with highly corrosive mediums. A systematic determination is being made of the behavior of the basic welding variables associated with the cone-arc process. The effects of arc-current magnitude and arc-current duration on cone-arc welds are described. The mechanical properties of high-temperature brazing alloys have been investigated, and the joint efficiency has been calculated by comparing the tensile strength of the brazed joint with the tensile strength of the parent metal that has undergone the same temperature cycle as that used in brazing.

The production of spherical particles of alloys of uranium with nickel, vanadium, columbium, and molybdenum is being studied. The methods being investigated are suspension in refractory powder and heating above the solidus, momentary melting while passing through an arc, and spraying from a metallizing gun. Tests on solid phase bonding are being made. The first group of samples has revealed that there is little variation in degree of bonding over a large temperature range.

The effect of small differences in test temperature on the stress-rupture life and creep rate of Inconel has been studied. The creep properties of Inconel when tested in argon and air have been studied, and it was found that Inconel tested in air has a much longer stress-rupture life than Inconel tested in argon.

The emphasis in dynamic corrosion testing in which thermal convection loops are used has shifted from testing fulinak 14 to testing various coolants and fuels containing zirconium fluoride. The coolants and fuels containing zirconium fluoride are not so corrosive as fulinak 14 is to Inconel. This is probably due to the more careful preparation and handling prior to the corrosion tests. With the zirconium fluoride fuels, the corrosion in the hot leg is approximately 5 mils after 500 hr of operation compared with the 10- to 15-mil depth of corrosion experienced when fulinak 14 was used.

The effect of different cleaning procedures on the corrosive action of the fluorides on Inconel is being studied. Static and modified dynamic tests have been used to determine the effect of time, temperature, and various additives on the corrosion behavior of the fluorides. It has been found that most of the corrosion occurs in the first 500 hr of operation. Strange results were obtained in the corrosion testing at extremely high temperatures – the amount of corrosion appreciably decreased. This was probably due to the formation of a thin film of uranium oxide on the surface of the test capsule. Addition of the strong getters has markedly decreased the corrosive action of the fluorides. The most striking example was the addition of zirconium hydride to the fulinak 14 that was circulated in a thermal convection loop. Upon examining the thermal convection loop after 500 hr at 1500°F, it was found that the loop suffered the least amount of attack of any thermal convection loop run with the fluorides, the maximum depth of attack was 0.5 mil.

Additional static and dynamic tests were run in an attempt to find inhibitors for the mass transfer and corrosion exhibited in the metal-hydroxide systems. Additional tests have shown that the mass transfer experienced in the nickel-hydroxide

system can be stopped by using purified hydrogen over the system.

The study of the compounds formed by the interaction of nickel in the hydroxides has shown the appearance of two new compounds – $NaNiO_2$ and $LiNiO_2$. These compounds, which have been called sodium nickelate(III) and lithium nickelate(III), have been identified by chemical analysis for nickel and the alkali metals, by several chemical reactions, including a quantitative determination of the oxidizing power and the reaction that gives a known trivalent nickel compound, and by complete crystal structure analysis.

CERAMICS RESEARCH

A ceramic coating has been successfully applied to nickel, and a nickel radiator assembly is being coated for the ANP Project. Work is continuing on the development of a fluoride-resistant coating. A ceramic coating containing 30 mole % boron has been successfully flame-sprayed on thin stainless steel plates for use in shielding studies. Preparation of a coated plate 5 ft square by $\frac{7}{8}$ in. thick, for shielding tests, is being undertaken.

A technique for the synthesis of hafnium carbide has been developed, and about 200 g of this material has been prepared for test. Hardness determinations of hafnium carbide indicate a Vickers hardness value of 2910 for this material, which is higher than the value for boron carbide. X-ray and chemical analyses of the material have been completed. The possibility of extruding thoria shapes for a breeder reactor is being evaluated. A novel material composed of glass-bonded beryllium oxide is proposed as a reflector moderator material, and preliminary test data have been obtained. X-ray photographs of thorium at 1500°C and hafnium oxide between 1400 and 1900°C have been made with the high-temperature x-ray camera.

A technique for preparation of a slurry from used magnesia crucibles was developed by the Engineering Department in connection with a feasibility study of a method for reclaiming waste fissionable material.

HRP METALLURGY

Continued assistance has been given to the HRP. Welding and fabrication specifications for stainless steel and pressure vessel steels are being written. Investigations of the properties and fabrication of titanium have continued.

FABRICATION RESEARCH

Production of enriched uranium fuel and control rod elements for operation of the MTR was maintained at an all-time high. Besides completion of the sixth and seventh reactor loadings, three new loadings of "sweetened" elements (168 g per unit) were fabricated according to specifications and delivered to Arco. Work on the eleventh and twelfth loadings is 90 and 60% complete, respectively. In the process improvement effort, two new techniques have been developed to increase the production output of these reactor components.

Experimental fabrication studies have been initiated to modify the present MTR fuel and control rod element for improved operational performance. Experiments designed to check whether brazing flux is being entrapped during fabrication and the extent to which its presence would poison the reactor were conducted. Analysis of a solution resulting from dissolving a dummy aluminum assembly indicated that the unit contained 1.26 g of lithium, which would reduce $\Delta k/k$ by a factor of 2.7% in the MTR lattice. A critical experiment in the BSR on an MTR fuel assembly in the unbrazed and the brazed condition showed the difference to be equivalent to 30.8 g of gold, or a loss in $\Delta k/k$ of approximately 3%.

Possible design changes in the construction of the MTR fuel element have been analyzed in an effort to reduce the V_{H_2O}-to-V_{Al} ratio to less than 0.60. A new active unit with 19 plates has been successfully fabricated that has a V_{H_2O}-to-V_{Al} ratio of 0.56 compared with 0.72 for the present fuel unit.

Several replacement fuel and control rod elements were fabricated for service in the LITR.

PHYSICAL METALLURGY OF REACTOR MATERIALS

E. J. Boyle

ALLOY DEVELOPMENT

J. A. Milko

The investigation of thorium alloys has continued. For the probable future use of thorium in a breeder type of reactor, it will be necessary that this material possess satisfactory corrosion resistance, dimensional stability, and perhaps high strength. It seems that in order to improve the corrosion properties of thorium, it must be alloyed, preferably to obtain a solid solution type of alloy.

Recently, individual additions of columbium, vanadium, and molybdenum have been made to Ames thorium. These alloys were prepared by induction melting in a furnace described in ORNL-1090.[1]

The cast alloy billet, approximately 1⅛ in. in diameter and 5 in. long, was swaged through a series of dies to a ⅝-in.-dia rod. Four ⅜-in. test bars were usually machined from each rod. These were then annealed in a vacuum for ½ hr at 750°C and then tested in tension by conventional methods at a strain rate of 0.05 in./min. The data thus obtained are given in Tables 1 and 2.

Effect of Columbium on the Strength Properties of Ames Thorium. The addition of columbium to Ames thorium produces definite changes in the strength properties of the thorium, as shown in Table 1. The columbium additions of about 0.25% appear to strengthen the thorium. Direct comparison with the effect of carbon additions cannot be made because Ames metal with similar carbon content was not available. It is believed that this strengthening effect amounts to 8,000 to 10,000 psi in the proportional limit, yield strength, and tensile strength. The ductility appears to be lowered by this addition. This behavior is suggestive of solid solution hardening.

The addition of 0.5 and up to 2% columbium definitely lowers the strength properties of the Ames metal, with corresponding increases in ductility. This pattern of behavior appears to be associated with either a deoxidation action of the columbium or with a carbide formation. In other alloys, columbium may function as both a strong deoxidizer and a carbide former.

Additions of 4 and 8% columbium seem to increase the strength properties over those of the 2% alloy. The ductility tends to be lowered by these additions. This behavior is suggestive of a eutectic or compound formation.

The foregoing tentative conclusions will be more fully evaluated later. Microscopic examination and hardness measurements may improve the understanding of the behavior. It may be necessary to

[1] D. E. Hamby, *Interim Report on Metallurgy of Thorium and Thorium Alloys*, ORNL-1090, Fig. 46, p. 53

TABLE 1. EFFECT OF COLUMBIUM ON THE STRENGTH PROPERTIES OF AMES THORIUM

INTENDED PERCENTAGE OF COLUMBIUM	TENSILE STRENGTH (psi)	YIELD STRENGTH AT 0.2% OFFSET (psi)	PROPORTIONAL LIMIT (psi)	ELONGATION IN 1.5 in (%)	REDUCTION OF AREA (%)
0.00	25,200 to 41,700*	17,000 to 25,800	10,500 to 21,600	48 to 68	69 to 78
0.25	41,300	36,000	28,500	20.0	38.0
0.50	35,400	27,300	18,300	23.0	46.0
1.00	34,300	23,900	13,600	26.0	44.0
2.00	24,900	9,500	5,700	40.0	60.0
4.00	30,100	13,100	7,500	33.0	59.0
8.00	33,200	13,400	6,600	29.0	50.0

*Determined on Ames thorium billets, with various carbon contents, extruded at 950°C from a 3-in. to a ⅝-in. diameter and annealed at 750°C for ½ hour.

TABLE 2. EFFECT OF VANADIUM ON THE STRENGTH PROPERTIES OF AMES THORIUM

INTENDED PERCENTAGE OF VANADIUM	TENSILE STRENGTH (psi)	YIELD STRENGTH AT 0 2% OFFSET (psi)	PROPORTIONAL LIMIT (psi)	ELONGATION IN 1.5 in. (%)	REDUCTION OF AREA (%)
0.00	25,200 to 41,700*	17,000 to 25,800	10,500 to 21,600	48 to 68	69 to 78
0 25	30,900	20,000	16,200	47	57
0.50	29,300	17,900	13,700	57	64
1 00	27,400	16,600	13,700	51	62
2 00	33,600	16,300	11,400	34	55
4.00	39,500	20,400	12,100	26	40
8 00	36,700	20,200	12,700	28	50

*Determined on Ames thorium billets, with various carbon contents, extruded at 950°C from a 3-in diameter and annealed at 750°C for ½ hour

use x-ray methods to determine solubility variations in the several columbium-thorium alloys.

Effect of Vanadium on the Strength Properties of Ames Thorium. An attempt was made to evaluate the effect of vanadium on the properties of Ames thorium, and the results are presented in Table 2. From the data of Table 2, it is evident that the addition of vanadium up to 1% tends to lower the strength properties of thorium. Beyond this amount, there appears to be a slight increase in the strength properties, with a slight increase in the ductility. Since it would be quite difficult to evaluate this behavior in terms of solubility and compound or eutectic formation without additional study, these alloys will be studied further by metallographic methods.

Effect of Molybdenum on the Strength Properties of Ames Thorium. No reliable data can be presented on the effect of molybdenum on the strength of Ames thorium. In the preparation of these alloys, it was observed that the solution of this element in thorium is quite difficult in the temperature range of 1700 to 1800°C. The dilute alloys, when cast, were unsound. The swaged rounds from such billets were likewise unsound in certain portions. Only one or two sound test bars were obtained from this series of dilute alloys. For that reason, no conclusions can be drawn as to the effect of molybdenum. Another attempt will be made to obtain satisfactory alloys.

PHYSICAL PROPERTIES OF THORIUM

R. E. Adams

The electrical resistance furnace previously described[2] is being used in the studies of the physical properties of thorium. In this furnace, thorium rod specimens are heated by self-resistance, a low-voltage, high-amperage current is passed through the specimen. Temperature is measured optically at a small hole drilled radially at the center of the rod. The melting point, electric resistivity, and thermal expansion at high temperatures are being studied.

Melting Point Tests. The melting point is measured by observing the temperature at the instant melting occurs around the small sight hole. Melting points of pure iron and pure nickel rods determined by this method have ranged between 10 and 25°C below the accepted values. Melting points of Ames thorium rods have ranged between 1700 and 1755°C. A single value of 1755°C has been obtained on a rod of iodide thorium. With thorium, it is difficult to determine the exact instant of melting, and further work will be done in an effort to improve the accuracy of the melting point determinations.

Electric Resistivity of Thorium. The electric resistivity of thorium is measured across a ½-in. length at the center of the test specimen. When

[2] R E Adams, *Met Quar Prog Rep July 31, 1952*, ORNL-1366, p 10

electric resistivity is plotted as a function of temperature, a sharp increase in resistivity occurs at temperatures ranging between 1350 and 1435°C. Figure 1 shows such a curve for iodide thorium, in which the average resistivity of the center ½ in. of the rod is plotted against the observed temperature at the center of the rod. Similar data have been obtained with Ames thorium rods. The temperature at which resistivity starts to increase and the steepness of the curve at the break differ slightly among specimens from different billets of thorium. Further work is being done to study these effects.

X-ray diffraction studies, reported in detail in the Ceramics Research section, indicate the possibility of an allotropic transformation in thorium in the vicinity of the temperature at which the abrupt increase in electrical resistivity occurs. The crystal structure of thorium appears to be unchanged at the higher temperatures, but there is a large increase in the lattice parameter. These results will be checked with more exact measurements on iodide thorium.

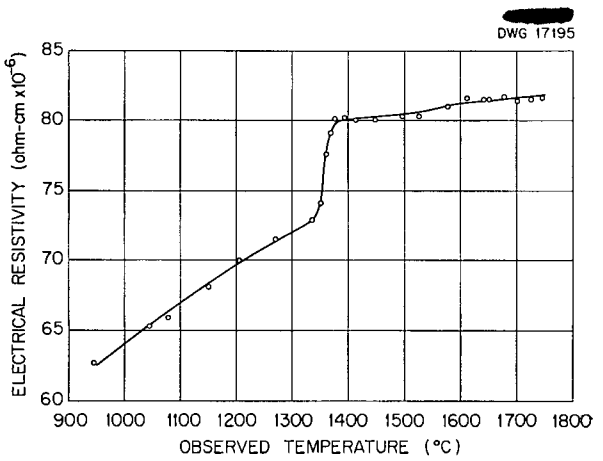

Fig. 1. Electrical Resistivity of Iodide Thorium.

Thermal Expansion of Thorium. The electrical-resistance furnace is also being used to study the thermal expansion of thorium at high temperatures. For these tests, the change in length between marks 1 in. apart at the center of the specimen has been measured with a micrometer microscope. Preliminary tests indicate that the length of thorium increases approximately linearly with temperature between about 900 and 1600°C. Additional tests will be made to verify these results.

RECRYSTALLIZATION

F. H. Eckert

Recrystallization experiments have been completed on thorium-carbon alloys. Four iodide thorium melts with intended carbon contents of 0.05, 0.07, 0.09, and 0.11% were prepared in an inert-atmosphere arc furnace. The resulting thorium buttons were cold rolled approximately 40%, homogenized at 1275°C for 12 hr in an argon atmosphere, and then cold-rolled 70% to 0.07-in.-thick plates. These plates were cut into 0.4-in.-square specimens and isothermally annealed for 1 hr at temperatures ranging from 500 to 740°C. The progress of recrystallization was traced by Vickers hardness measurements and metallographic examination.

Table 3 shows the carbon, nitrogen, and oxygen analyses for these alloys. Oxygen and nitrogen increased with increasing carbon content, and it is believed that this is due to contamination by the master alloy, since all fabricating procedures were identical except for greater addition of the master alloy to the higher carbon content alloys.

Table 4 shows the annealing temperature at which recrystallization starts and finishes for the

TABLE 3. ANALYSES OF CARBON-THORIUM ALLOYS

SAMPLE NO.	CARBON		NITROGEN (%)	OXYGEN (%)
	Intended %	Actual %		
5	0 13	0.134	0.06	0.05
6	0.11	0.10	0 007	0.04
7	0 09	0 085	0 004	0 02
8	0 07	0 049	0.001	0.01

various carbon contents. These temperatures were determined by metallographic examination. Figure 2 shows the effect of carbon on the recrystallization of thorium. The addition of carbon up to 0.13% apparently has no significant effect on the recrystallization temperature for iodide thorium. The reason for the slight rise in hardness from 675 to 740°C was not definitely determined, but it is thought that solid solution hardening may have been started by the carbon in the thorium.

TABLE 4. ANNEALING TEMPERATURES AT WHICH RECRYSTALLIZATION STARTS AND IS COMPLETED FOR VARIOUS CARBON-THORIUM ALLOYS

CARBON CONTENT (%)	ANNEALING TEMPERATURE (°C)	
	Recrystallization Starts	Recrystallization Complete
0.134	510 to 520	650
0 101	510 to 520	650
0 085	500 to 510	650
0 049	500 to 510	650

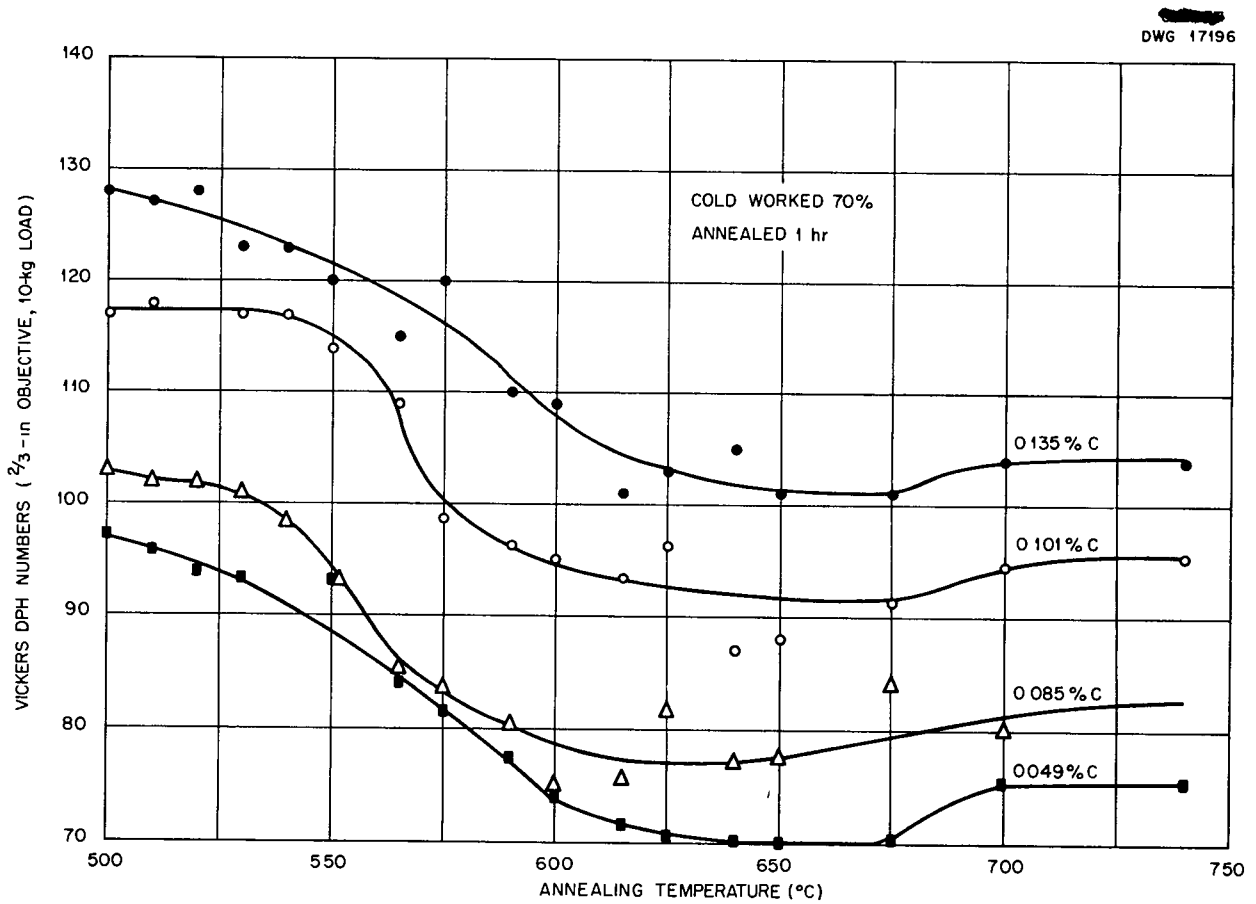

Fig. 2. Effect of Carbon on Recrystallization of Iodide Thorium.

ANP PROGRAM

W. D. Manly

WELDING AND BRAZING

G. M. Slaughter

ARE Welding. Procedure specifications for d-c inert-arc welding of Inconel pipe and fittings for use in highly corrosive mediums and the operator's qualification-test specification have been prepared for ARE fabrication. A manual, entitled *Joint Design for Inert-Arc Welded Vessels,* was prepared as an aid in construction of the ARE. This manual describes the preferable basic joint designs for use in pressure vessels that are to be operated at elevated temperatures in a severely corrosive environment.

Cone-Arc Welding. A topical comprehensive report of cone-arc welding research conducted at this laboratory is being written for publication as an unclassified ORNL report and as a paper for publication in the *Welding Journal and Research Supplement.* This report will discuss the basic principles of the cone-arc process, the actual physical set-up of the apparatus, and the extent of research on the welding of thin-walled tube-to-header joints.

During the research on the cone-arc welding of the 0.100-in.-OD stainless steel tubes with 0.010-in. wall thickness to the 0.125-in. stainless steel headers, it was noticed that many welds exhibited a two-pass appearance. An investigation of this phenomenon was made to obtain a better understanding of the mechanism of the cone-arc welding process. Figure 3 shows a microstructure in a cone-arc weld that resembles, in many ways, the structure resulting from a multiple-pass butt weld. There were apparently two stages of melting and growth of dendrites across the interface of the two regions.

The two-pass effect seems to result from the very rapid melting of the tube during the initial phases of the welding process. With the tube flush against the top header surface, the intense heat of the welding arc is at first centered on the thin-walled tube. The tube apparently melts along its length for a short distance until the thermal insulation of the very thin tube-to-header spacing is overcome. After this occurs, much of the heat is then used in melting the header material. At this time, conditions are reached that approach more nearly the equilibrium state. The lower pass is then that resulting from the initial phase of the welding, and the upper pass, represented by the molten weld pool, remains throughout the major portion of the welding cycle.

Since it would seem that the arc would play more directly upon the header sheet at the initial point of striking if the tube were recessed in the hole, this technique was employed in an attempt to eliminate the two-pass weld. Figure 4 shows a cone-arc weld in which the tube had been recessed 0.022 inch. Complete welding occurred and the two-pass effect was eliminated. It should be remembered that the two-pass weld is not considered as being detrimental but is merely a characteristic of joints made under certain conditions.

Relatively long arc distances also tend to reduce the tendency for this type of joint. Apparently, as the arc distance increases, more of the arc beam impinges on the header sheet, and the drastic heating of the tube wall is minimized.

Fig. 3. Photomacrograph of a Stainless Steel Tube-to-Header Cone-Arc Weld Exhibiting the Two-Pass Appearance. Etched with Aqua regia. 18X

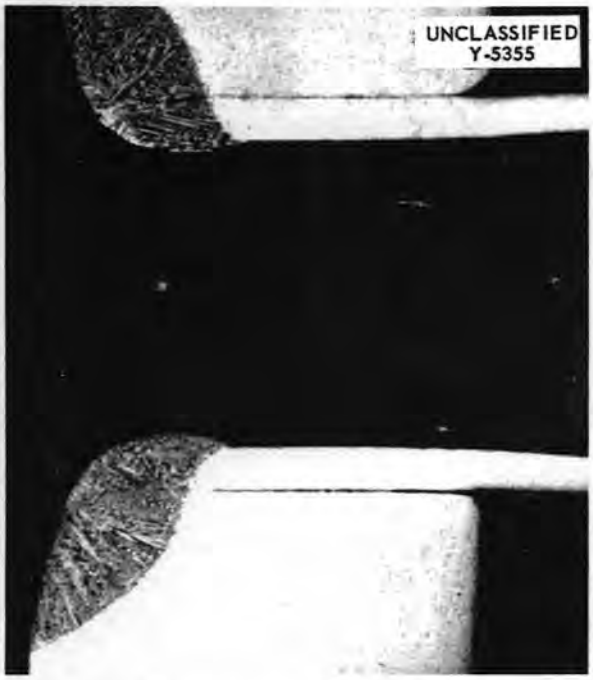

Fig. 4. Photomacrograph of a Stainless Steel Tube-to-Header Cone-Arc Weld Showing the Effect of Recessing the Tube Upon the Elimination of the Two Passes. Etched with aqua regia. 18X

Resistance Welding. Since it is desirable to determine the feasibility of electrical-resistance spot welding of stainless steel clad fuel elements to both themselves and to stainless steel sheet, an investigation is being made in which welding variables are controlled precisely. The preliminary experiments have consisted of spot welding fuel elements containing a core of 50% UO_2 and 50% Fe. One value of electrode force was used to make welds at a series of welding currents in an attempt to determine the magnitudes of current required to produce good weld penetration without materially affecting the core structure. Figure 5 shows a spot weld made in a 0.030-in. fuel element under 600 lb of electrode force and 6200 amp of welding current. These conditions sometimes result in very slight weld porosity, but it can be seen that excellent weld penetration is obtained. It is expected that the use of slightly higher values of electrode force will eliminate the tendency toward weld porosity. When optimum conditions have been determined, tensile strengths of lap joints will be measured.

Brazing. Although the 60% Pd–40% Ni brazing alloy has many very desirable properties, its high

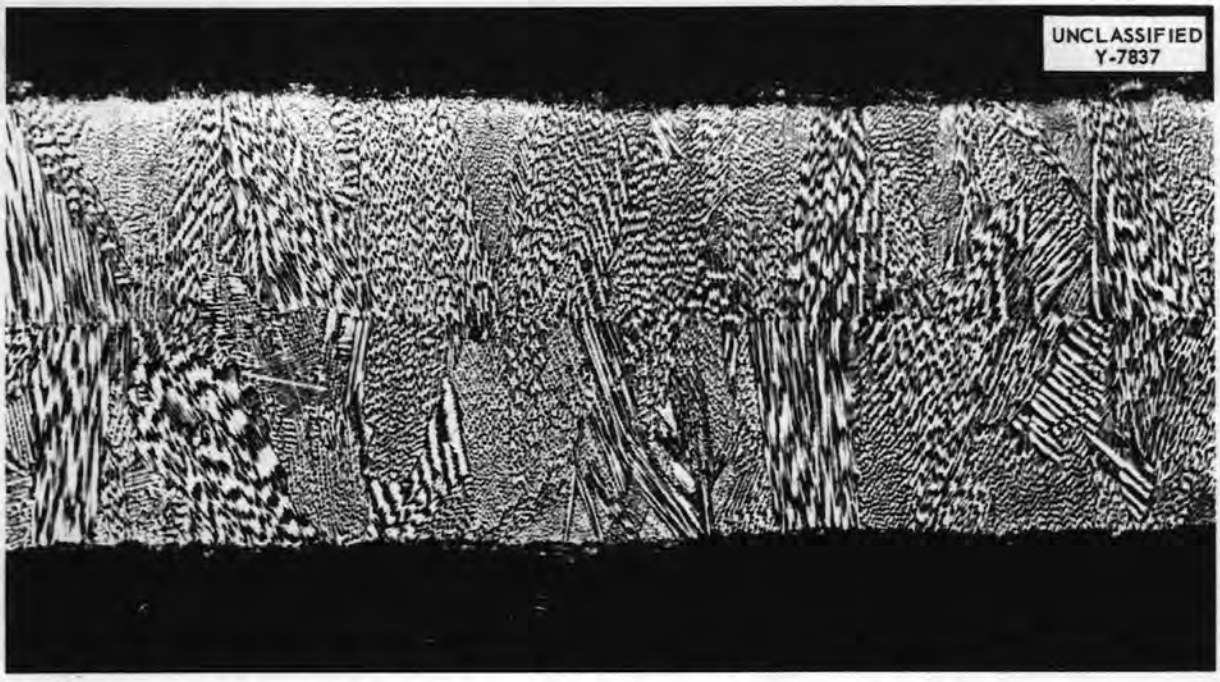

Fig. 5. Spot Weld Between Two Stainless Steel Clad Fuel Elements. Excellent weld penetration is present. The spot welding conditions were: electrode force, 600 lb; weld time, 5 cycles; welding current, 6200 amperes. Etched with aqua regia. 100X

melting point might possibly exclude its use in many applications. In an attempt to lower its melting point by alloying, beryllium additions from 0.25 to 4% were made. A 1% Be alloy was found to have a melting point slightly below 2200°F, but recent tests indicate that its flowability properties are very poor. Aluminum and copper additions will be used in an alloy development program for further attempts to obtain a brazing alloy with a lower melting point without impairment of the corrosion resistance and physical properties of the basic palladium-nickel alloy.

Results on the room-temperature tensile strengths of Inconel butt-joints brazed with Nicrobraz alloy seem to indicate that short brazing times of 10 min or less lead to the production of weak joints. Samples held at the brazing temperature for 20 min seem to produce stronger joints. Figure 6 shows the room temperature fracture of a joint held at the brazing temperature for 5 minutes. Some Nicrobraz can be seen in this photograph, but there is no evidence of brittle fracture. Although the specimen that was held for 20 min at the brazing temperature broke near the brazed joint, no evidence of Nicrobraz alloy could be found upon metallographic sectioning. This greater alloying of the braze and base metals is a result of the increased diffusion occurring during the longer period. The increase in tensile strength of the second bar probably results from this alloying.

The average value obtained from four room-temperature tensile strength tests of joints brazed for short times was 38,300 psi. A joint brazed for 20 min at the brazing temperature fractured at 81,700 psi. The average tensile strength of four Inconel bars that were heat-treated in the same manner as the tensile bars was 87,300 psi. This seems to indicate that if time is allowed for sufficient diffusion to occur, joint efficiencies of over 90% can be obtained. A more thorough investigation of brazing times is being conducted.

The tensile strengths of Nicrobrazed Inconel joints tested at 1500°F were much more consistent. The average tensile strength of joints brazed for short times was 24,400 psi, whereas the sample brazed for 20 min fractured at 24,700 psi. Several test bars of the parent metal failed at a point definitely not in the diffusion zone of the brazed

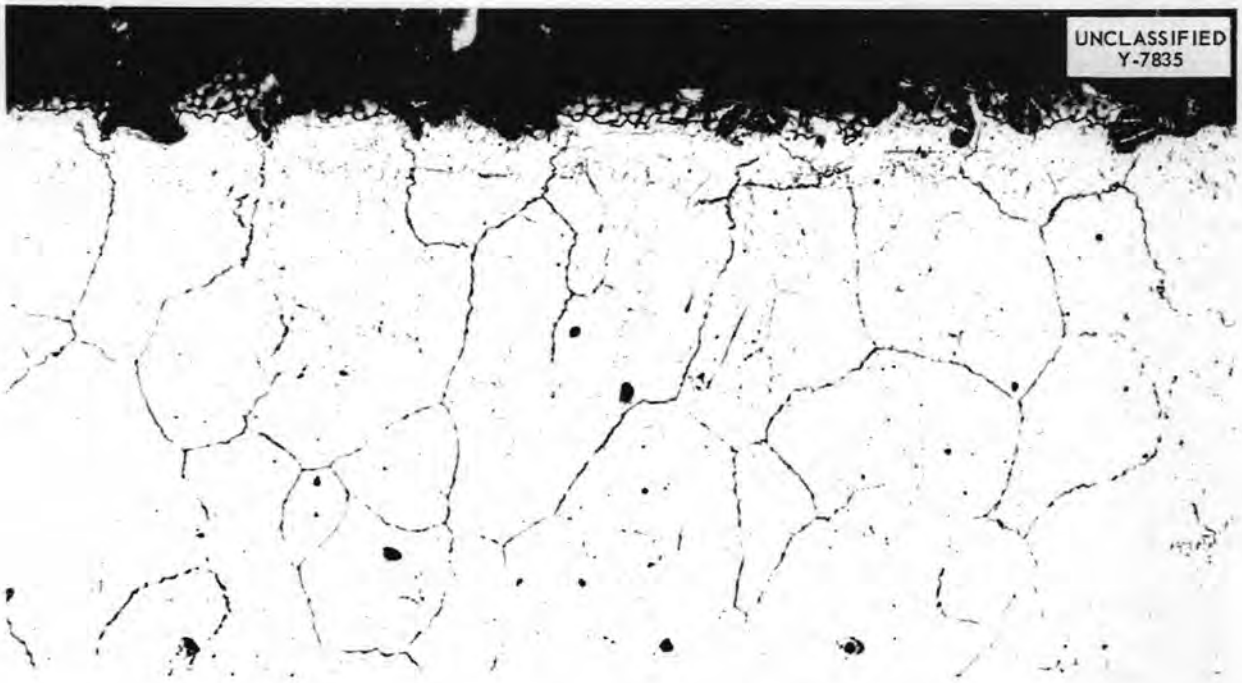

Fig. 6. Fracture of a Nicrobrazed Inconel Test Bar that Had Been Held for 5 min at the Brazing Temperature. The fracture occurred at the braze metal–Inconel diffusion Zone. Etched with aqua regia. 250X

joint. The average elevated-temperature tensile strength of four Inconel test bars, which were heat-treated at the brazing temperature for 5 min, was 23,700 psi. These data indicate that the Nicrobrazed Inconel joints at 1500°F are often as strong as the Inconel base metal. The diffusion of the braze metal while the specimen is at the testing temperature undoubtedly has some effect on the joint strength at this temperature.

Since A nickel is relatively unattacked by molten sodium hydroxide at 1500°F, it was thought advisable to test the corrosion resistance of nickel joints brazed with several of the more promising alloys. Figure 7 shows a joint brazed with the 60% Pd–40% Ni alloy and tested in sodium hydroxide for 100 hr at 1500°F. It can be noted that no attack is present. Other alloys, such as the 75% Ag–20% Pd–5% Mn, shown in Figure 8, were heavily attacked. A nickel joints brazed with the 16.5% Cr–10.0% Si–2.5% Mn–71.0% Ni and the 16.5% Cr–10.0% Si–73.5% Ni alloys fractured during removal from the test capsule.

Joints of Inconel, type 316 stainless steel, and A nickel were prepared with most of the brazing alloys currently being investigated. High-temperature oxidation studies at 1500°F were then conducted, and the amount of oxidation was determined metallographically. The 60% Pd–40% Ni alloy was unattacked when in contact with the three base metals tested. The Inconel joint is shown in Fig. 9. The effect of base metal composition on corrosion can be illustrated by Figs. 10 and 11. Figure 10 shows an Inconel high-temperature oxidation specimen brazed with 64% Ag–33% Pd–3% Mn alloy, and Fig. 11 shows a type 316 stainless steel specimen brazed with the same alloy. The Inconel braze is slightly pitted, but the stainless steel braze is extremely heavily attacked. The opposite effect appears to be the case when the same base metals are brazed with a 16.5% Cr–10.0% Si–73.5% Ni alloy. Figure 12 shows an Inconel joint exhibiting moderate attack on the brazing alloy, and Fig. 13 represents an unattacked stainless steel joint. One theory that might explain these phenomena is that the least corrosion-resistant constituents of the brazing alloy may diffuse more readily into certain base metals than into others and thereby increase the corrosion resistance of the joint.

Because brazing operations may be proposed for assembling fuel plates into subassemblies for certain types of reactors, it is of interest to study the static corrosion resistance of brazed joints in contact with sodium or lithium. Although testing and examination are not complete, some preliminary results have been obtained. Nicrobrazed joints on Inconel and type 316 stainless steel are relatively unattacked by sodium. Figure 14 shows the Inconel joint after contact with sodium, and Fig. 15 shows a stainless steel joint after it was tested in the same medium. Shown in Fig. 16 is a stainless steel joint brazed with the 16.5% Cr–10.0% Si–2.5% Mn–71.0% Ni alloy and tested in sodium. It can be noted that the brazing alloy is attacked only very slightly, but the cracking tendencies of this alloy are serious. The 16.5% Cr–10.0% Si–73.5% Ni alloy has a similar appearance under the same testing condition.

Several copper-base brazing alloys have been prepared for use in an investigation on the brazing of copper to Inconel joints for operation at a service temperature of 1500°F. Copper-beryllium, copper-silicon, and copper-tin alloys are being studied at present, and additions of other alloying elements will be examined. Melting point determinations, flowability tests, and tensile strength tests of joints at room and elevated temperatures are proposed for the determination of alloy suitability.

FABRICATION

E. S. Bomar J. H. Coobs
H. Inouye

Solid Fuel Formed in Spheres. A suggested geometry for the fuel in the Pratt and Whitney supercritical water reactor is that of spherical particles 0.010 in. in diameter. After these particles received a 6-mil protective nickel plate, they would be packed in beds in the reactor core, with cooling water flowing through the interparticle channels.

Several methods of preparation that involved the use of both high- and low-melting-point alloys were given a preliminary examination. Five per cent of uranium in molybdenum was used for the high-melting-point alloys, and 5% of uranium in nickel or copper was used for the low-melting-point alloys. The results showed only partial success. The methods investigated included

1. suspension in refractory powder and heating above the solidus,
2. momentary melting while passing through a carbon or tungsten arc,

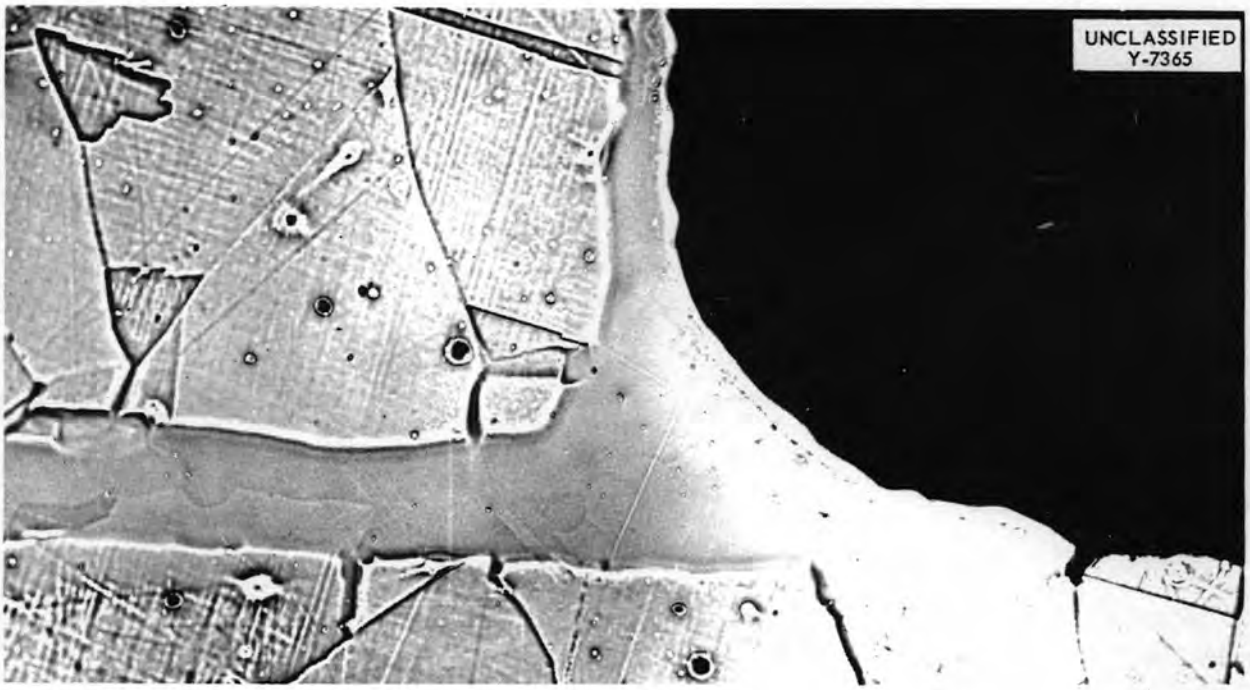

Fig. 7. A Nickel T Joint Brazed with 60% Pd–40% Ni Alloy and Tested in Sodium Hydroxide for 100 hr at 1500°F. There is no evidence of attack on the braze metal. Etched with KCN + $(NH_4)_2S_2O_8$. 150X

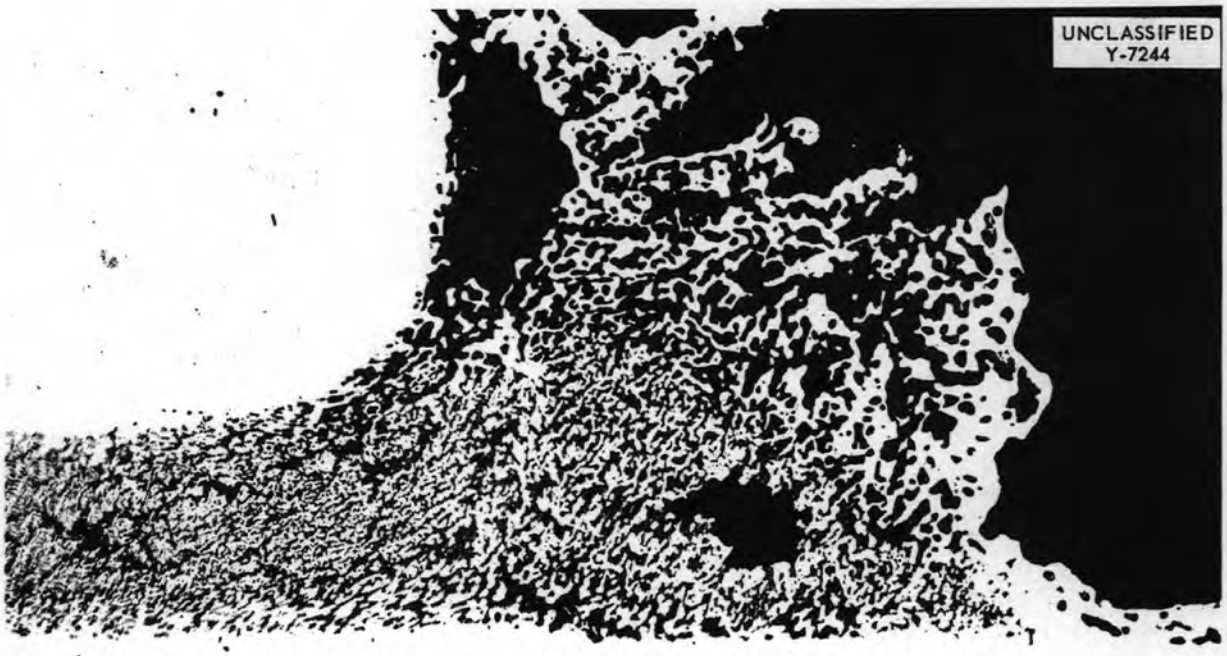

Fig. 8. A Nickel T Joint Brazed with 75% Ag–20% Pd–5% Mn Alloy and Tested in Sodium Hydroxide for 100 hr at 1500°F. Severe attack has occurred. Unetched. 150X

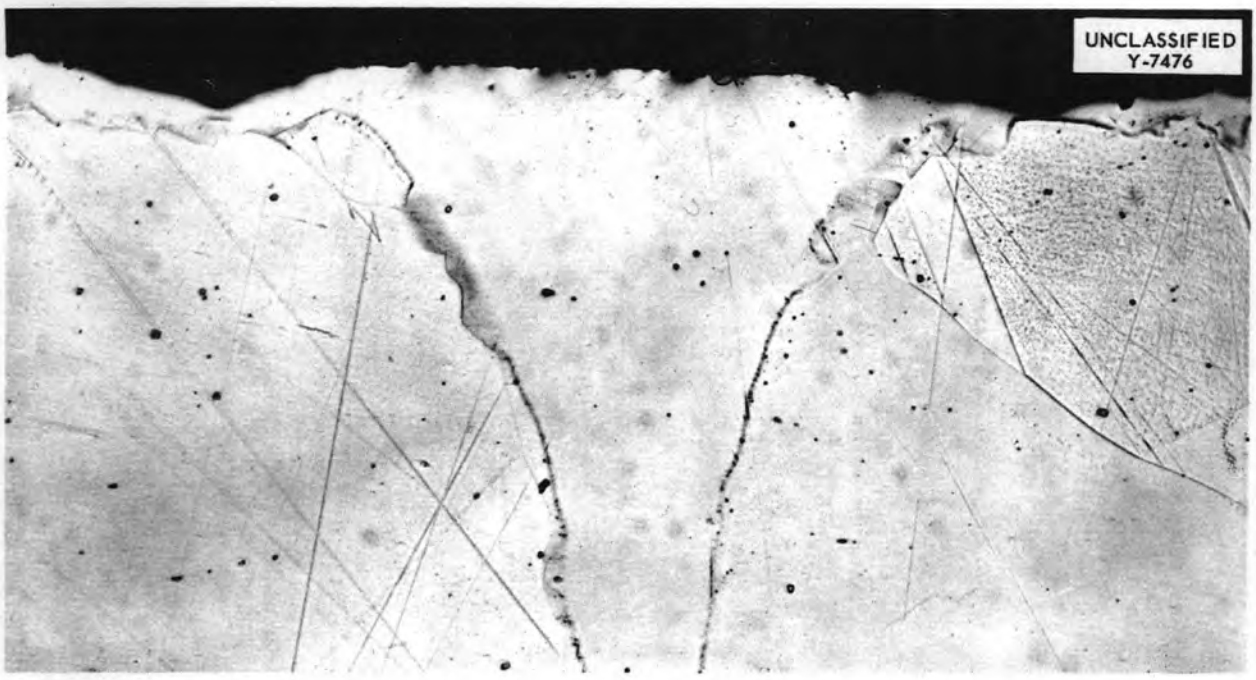

Fig. 9. Inconel Brazed with 60% Pd–40% Ni and Subjected to a High-Temperature Oxidation Test at 1500°F. No attack can be seen. Etched with KCN + $(NH_4)_2S_2O_8$. 200X

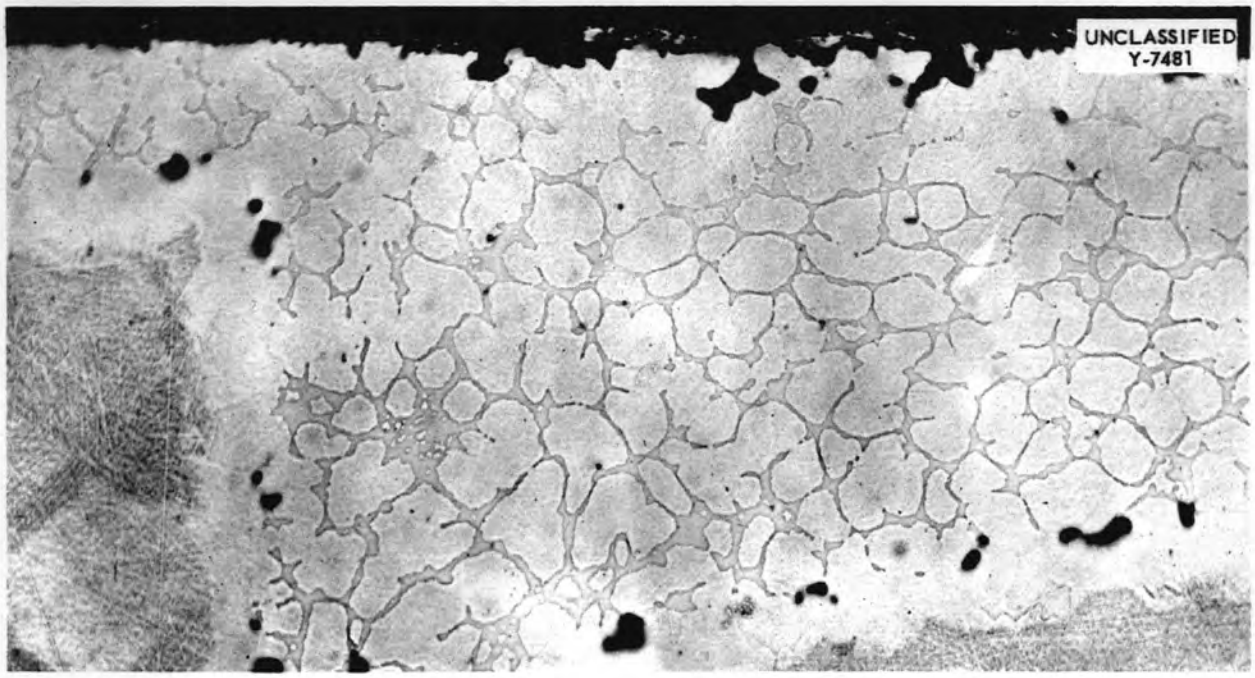

Fig. 10. Inconel Brazed with 64% Ag–33% Pd–3% Mn Alloy and Subjected to a High-Temperature Oxidation Test at 1500°F. Slight pitting attack can be seen. Etched with aqua regia. 200X

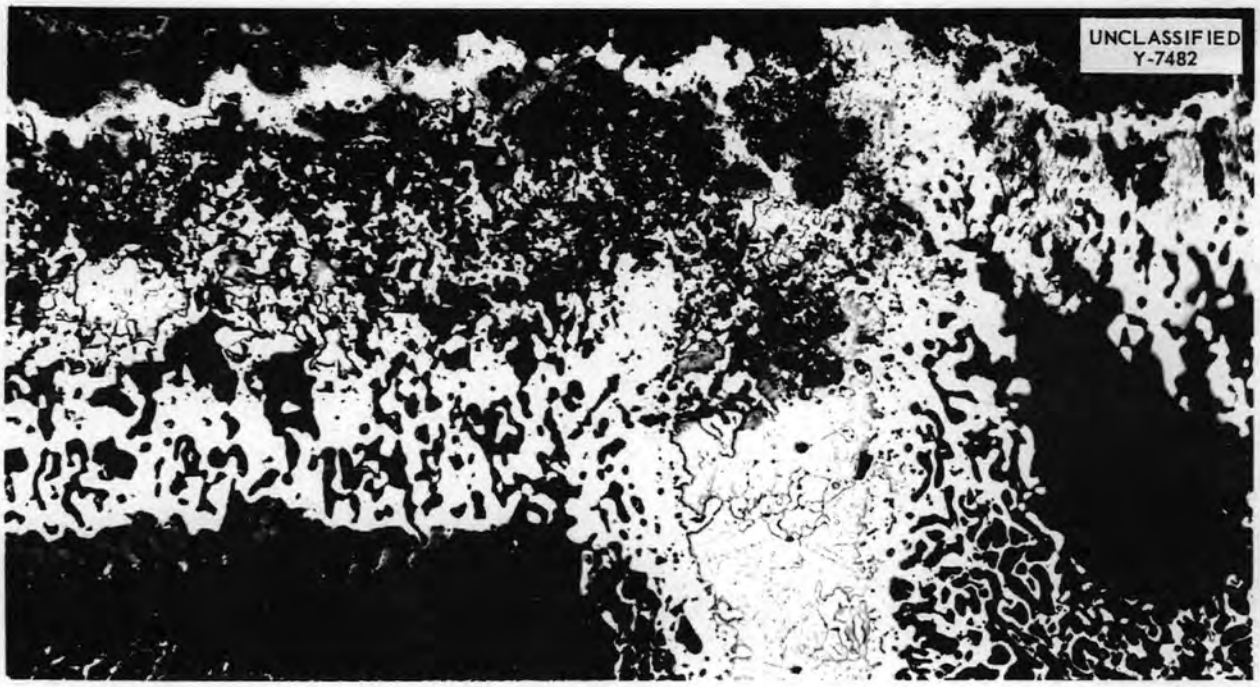

Fig. 11. Type 316 Stainless Steel Brazed with 64% Ag–33% Pd–3% Mn and Subjected to a High-Temperature Oxidation Test at 1500°F. Slight pitting attack can be seen. Etched with aqua regia. 200X

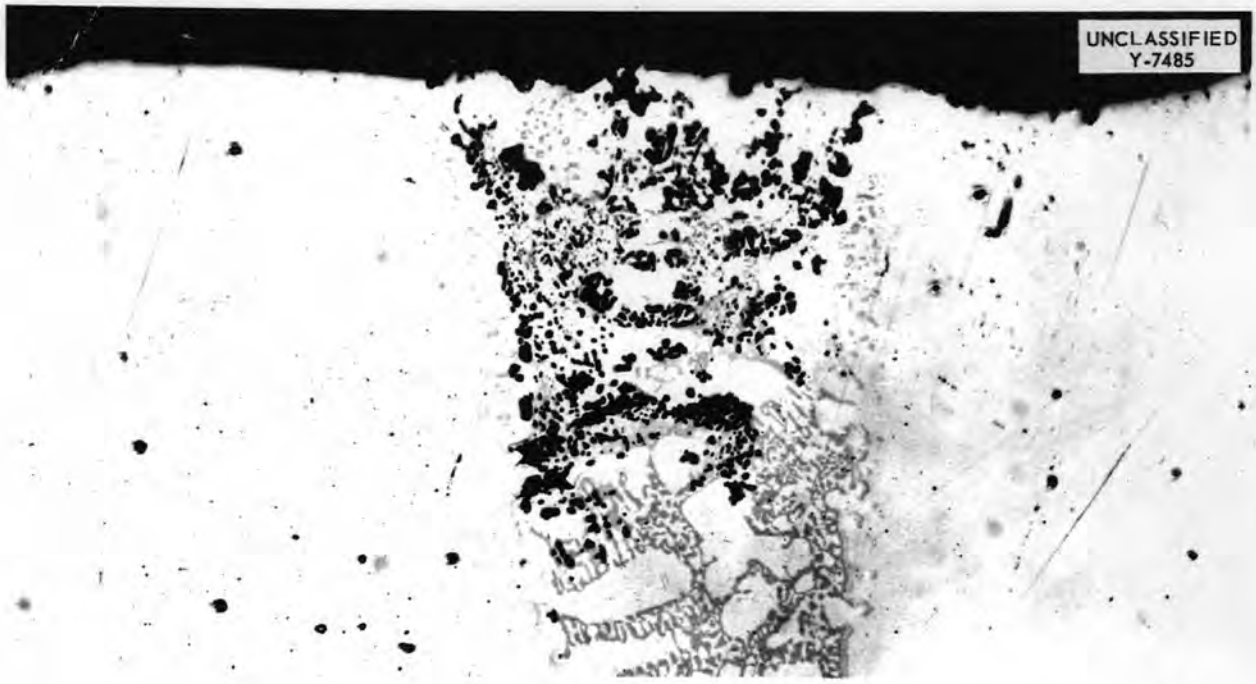

Fig. 12. Inconel Brazed with 16.5% Cr–10.0% Si–73.5% Ni and Subjected to a High-Temperature Oxidation Test at 1500°F. Slight oxidation of the brazing alloy can be seen. Unetched. 200X

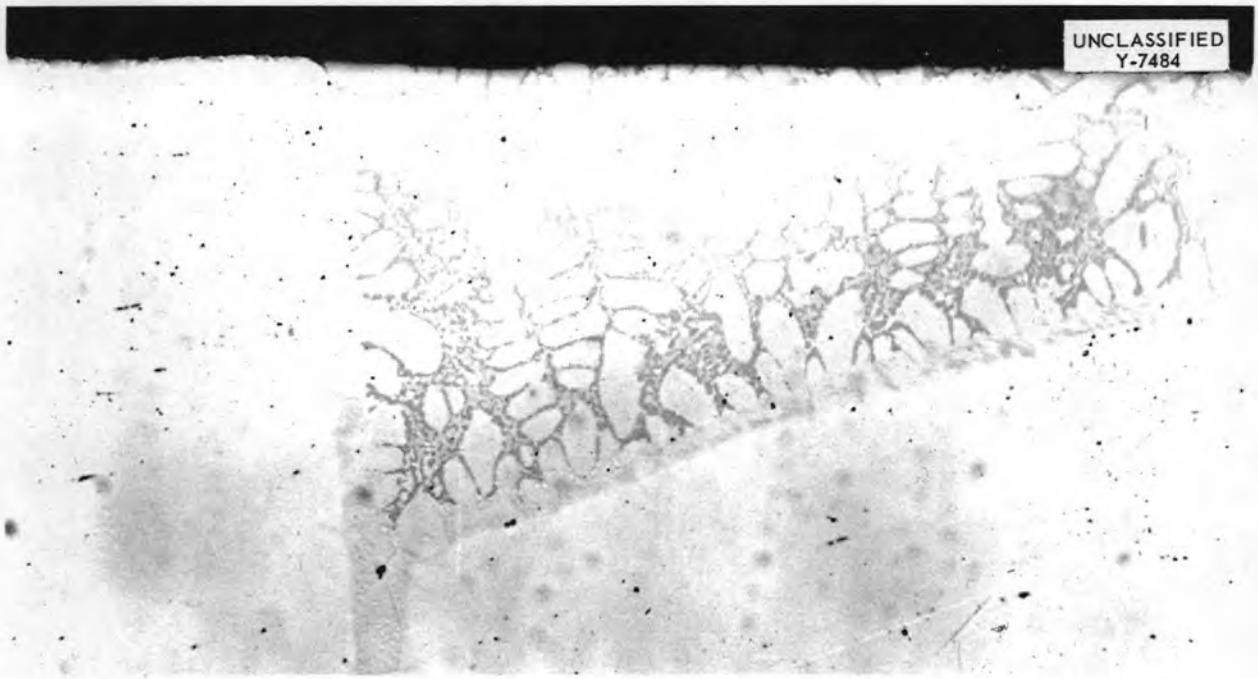

Fig. 13. Type 316 Stainless Steel Brazed with 16.5% Cr–10.0% Si–73.5% Ni and Subjected to a High-Temperature Oxidation Test at 1500°F. No attack present. Unetched. 200X

Fig. 14. Nicrobrazed Inconel Joint After Being Tested in Sodium for 100 hr at 1500°F. Joint relatively unattacked. Unetched. 150X

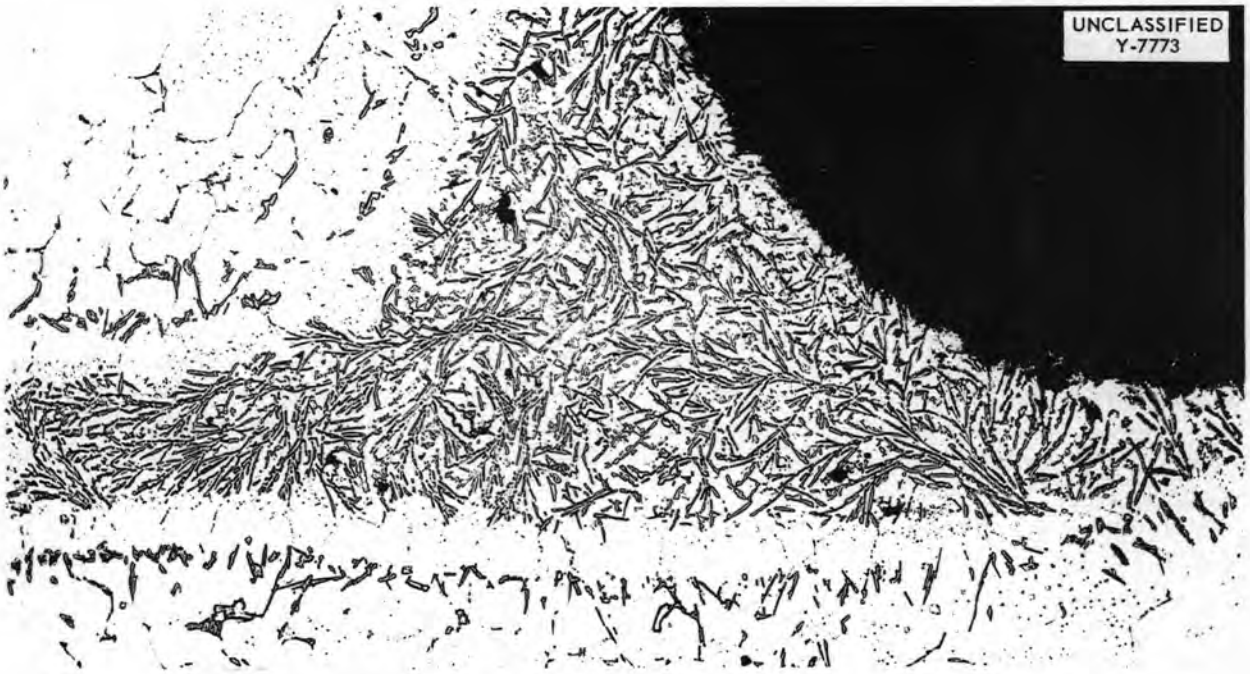

Fig. 15. Nicrobrazed Stainless Steel Joint After Being Tested in Sodium for 100 hr at 1500°F. No attack evident.

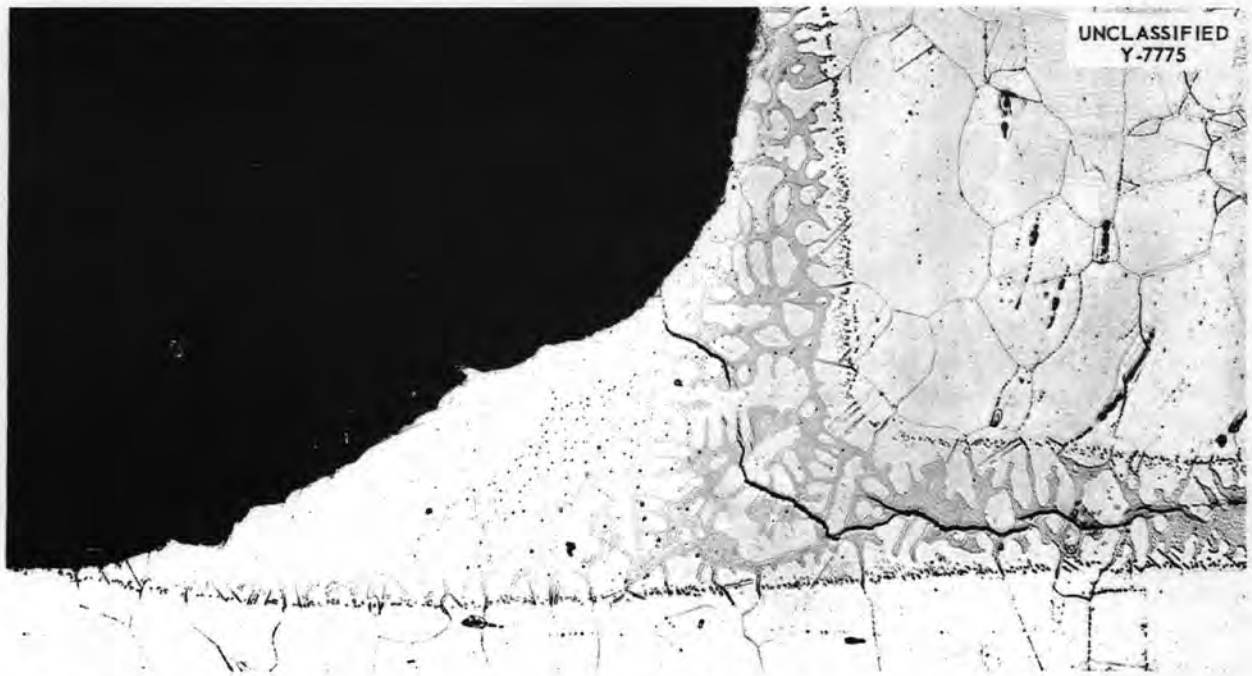

Fig. 16. Stainless Steel Joint Brazed with 16.5% Cr–10.0% Si–2.5% Mn–71.0% Ni Alloy and Tested in Sodium for 100 hr at 1500°F. Only very slight attack is present, but the cracking tendencies of the alloy are severe. Etched with aqua regia. 150X

3. momentary melting while passing through an atomic-hydrogen arc,
4. spraying from metallizing gun.

Suspension in Refractory The uranium-nickel and uranium-copper alloys were swaged and drawn to 0.010 in. in diameter, and then short segments were cut from them. The uranium-nickel particles were mixed with Al_2O_3, one sample was heated to 1450°C in hydrogen and the other was heated in vacuum (3 μ) to the same temperature. The uranium-copper particles were spread on a refractory plate and heated to 1100°C for 5 min in hydrogen. A surface film formed in all three cases and prevented spheroidization, even though a liquid phase was present.

Momentary Melting in a Carbon or Tungsten Arc. A rig was assembled to house two water-cooled electrodes, and the assembly was supplied with an argon atmosphere. Uranium-nickel alloy particles, similar to those used in the first method, were dropped through an arc struck between the electrodes. Alignment proved very critical, but the particles that passed through the arc zone did melt. The yield was quite low, however. The particles that passed through the carbon arc were porous, whereas those that passed through the tungsten arc were not.

Momentary Melting in Atomic-Hydrogen Arc Feed material of uranium-nickel alloy, similar to that used in the first method, was dropped through an atomic-hydrogen arc, and a small number of essentially spherical but porous particles was formed.

Spraying from a Metallizing Gun A length of 0.057-in. dia uranium-nickel wire was fed through a metallizing gun, and the resulting particles were collected in water. As with the other methods, a porous product resulted. Substitution of argon for the normal air blast produced what appeared to be a sound product, with only a superficial surface film.

During the process of dropping segments of wire through the tungsten arc, it was noted that small particles were ejected from the electrode at current densities high enough to melt the electrode tip. The bulk of the particles ranged in size from 0.010 to 0.020 inch. These results were duplicated when uranium-molybdenum electrodes were substituted for the tungsten electrodes. The uranium-molybdenum electrodes were prepared by pressing a mixture of the elemental powders and sintering at 1200°C for 5 hr in a vacuum of 0.5 to 1 micron. The spheroidized particles did not give a response on exposure to an alpha counter as did the parent electrodes and uranium-nickel particles from an earlier spraying experiment.

Solid-Phase Bonding. Tests are being made to determine which materials are easy to bond and which are difficult to bond. The initial tests, performed essentially as a screening operation, have been completed. They were run on both sheet stock and sintered powder compacts and were performed by stacking wafers in a molybdenum-lined graphite die. The laminates were hot pressed for 5 min at 3000 psi and at temperatures of 1150, 1200, and 1250°C in an argon atmosphere. Further tests have been run at 1150°C for 1, 10, and 30 min to determine the effect of time on the extent of bonding. Evaluation of these tests is not complete.

Examination of the first group of samples revealed little difference in the degree of bonding at the various temperatures. As was expected, considerably more diffusion occurred at 1250°C, but bonding was very little better.

In general, the various couples may be divided into four groups on the basis of the extent of bonding *excellent*, interface almost obliterated, inseparable, *good*, interface well defined, inseparable, *fair*, separated with some difficulty, *poor*, only superficial bonding. The couples studied fall into these categories in the following manner

Excellent
- Nickel to Inconel
- Nickel to stainless steel
- Stainless steel to stainless steel
- Iron to iron

Good
- Nickel to iron
- Nickel to nickel
- Molybdenum to nickel foil to molybdenum

Fair
- Molybdenum to nickel
- Molybdenum to Inconel
- Molybdenum to molybdenum

Poor
- Molybdenum to iron
- Molybdenum to stainless steel

The self-welding of the molybdenum, with or without a nickel-foil bonding layer, was poor at 1250°C, so supplementary runs were made at 1400 and 1500°C, with results as indicated above.

For molybdenum to nickel and molybdenum to Inconel, there was a measurable amount of diffusion

but only fair bonding, possibly because of the formation of a third phase of poor strength at the interface. Extensive diffusion (2 to 3 mils) occurred between molybdenum and iron and between molybdenum and stainless steel, but there was even less bonding than was found between molybdenum and nickel or between molybdenum and Inconel.

Further work with the use of electrodeposited chromium as a bonding layer is being done on the bonding of molybdenum to the other metals. Chromium is reported to be completely miscible with molybdenum and may be more compatible with the other materials.

Several small fuel assemblies have been prepared by using the electroformed nickel screen, filling with mixtures of UO_2 and stainless steel powder, and pressing rubberstatically. This step is followed by cladding both sides with iron or nickel sheet and hot pressing at 1250°C. The assemblies are now being examined for fuel distribution and bond integrity.

MECHANICAL TESTING

R. B. Oliver J. W. Woods
D. A. Douglas K. W. Reber

Uranium. Creep tests at 500°C in vacuum have been completed on beta-treated uranium (80 sec at 730°C, water quenched) at stresses of 5500, 4500, 4000, and 3500 psi. Tests are being made at the following stresses 2500, 2250, 2000, and 1500 psi.

When the tests now being made are completed, a design curve for the beta-treated uranium can be constructed, and the testing phase of the creep-of-uranium program will be completed. Thus far, the data indicate that the beta treatment and its accompanying increase in grain size increase the rupture life by a factor of about 3, and the creep rate is reduced to less than one-third the rate for the same material rolled at 600°C.

Thorium. During the past year, Ames thorium with a nominal carbon content of 0.040% and extruded at about 35 ft/min has been tested in vacuum at 300°C. The stress levels studied ranged from 16,000 up to about 22,000 psi, which is nominally the ultimate tensile strength. At stresses less than 16,000 psi, the creep rates became vanishingly small. One undesirable characteristic was noted the initial extension, which was as high as 5% at 16,000 psi, was excessive.

The amount and type of prior deformation are thought to be major factors influencing the magnitude of the initial extension. This was indicated by testing a bar that had been previously strained 5% in tension at room temperature. This treatment reduced the initial extension to about one half that observed for an unstrained bar. To explore this field further, two extrusions were made from a billet chemically similar to the billet previously used. The extrusions were at rates of 2.32 and 588 ft/min, respectively.

Specimens from these two extrusions are now being tested. The early data indicate that the slowly extruded bar has a greatly increased tensile strength at 300°C and a decreased initial extension. The very rapidly extruded (588 ft/min) bar shows a greatly reduced tensile strength at temperature, and the initial elongation is lower than that observed for the extrusions made at 2.32 and 32 ft/min. It is thought that these comparative values can be correlated with the textures developed at the different extrusion rates.

Type 316 Stainless Steel. Eight tests of sheet specimens (0.063 in.) of type 316 stainless steel in fulinak 14 at 815°C have been completed. The tests were conducted at 7300, 6800, 6300, and 5800 psi for correlation with specimens (from the same sheet of material) that were previously tested in argon at these stresses. Comparison of the data obtained in these two mediums indicates that at 7300 psi the creep-rupture properties are similar. At the lower stresses the rupture life and the ductility are substantially reduced by the presence of the corrosive molten fluoride mixture. Tests are to be made at stresses above 7300 psi and below 5800 psi to further extend the comparison of the properties of the metal in the two mediums.

The results of tests made in this Laboratory in argon atmospheres have been compared with the published results of tests conducted in air by other laboratories. At stresses above 7000 psi, the rupture life in the two atmospheres is the same, within the limits of experimental accuracy. At stresses below 7000 psi, the rupture life in argon appears to be slightly shorter than that observed in air, although the difference is too small to be conclusive without detailed analysis.

Inconel. One Inconel chamber for stress-rupture testing of Inconel in a liquid environment has been completed and calibrated. This chamber will immediately be charged with fuzrna 27 (chemical

composition 72.5% ZrF_4–16.5% NaF–11% UF_4 by weight) to evaluate the creep-rupture properties of Inconel at 815°C in this environment. Materials have been ordered for converting the remaining six available testing units to Inconel chambers.

At stresses less than 5000 psi at 815°C, the rupture life of sheet (0.063 in.) Inconel is shorter than that observed for similar tests conducted in air. Two tests conducted in an atmosphere of hydrogen have had a rupture life much shorter than that observed in argon (Table 5).

Metallographic examination of the one Inconel specimen that ruptured during test in a hydrogen atmosphere shows that the specimen exhibits much more profuse intergranular cracking than previously noticed in specimens tested in argon.

Tensile Testing. The furnace, chamber, and extensometer for tensile testing at elevated temperatures in vacuum or controlled atmospheres have been completed. The calibration of this system is being delayed by the service testing for other groups. The variables being studied include varying spring loading by the bellows, loading by the bellows owing to departures from ambient pressure, and friction in the furnace support system.

TABLE 5. COMPARISON OF RUPTURE LIFE OF INCONEL TESTED AT 815°C IN AIR, ARGON, AND HYDROGEN

STRESS (psi)	RUPTURE LIFE (hr)		
	In Hydrogen	In Argon	In Air
3500	265	726	Over 2,500
2500	400 (est)	1400	10,000 (extrap)

DYNAMIC CORROSION

G. M. Adamson

The joint dynamic corrosion program of the Metallurgy Division and the ANP Experimental Engineering Section has continued. This dynamic corrosion work is still being carried out in large thermal convection loops. Results of the experiments with Inconel loops are tabulated in Table 6.

Considerable effort has been exerted to find an inhibitor for use with the fluorides. Zirconium hydride has produced very optimistic results with fulinak 14 but only fair results with fuzrna 27. NaK has given a slight improvement to both fuels but not enough to be useful. One of the loop problems is to remove oxide scale from the inside of the pipes. Circulating NaK and dry hydrogen have proved unsuccessful for this task. Another series of samples has been drilled from the inner pipe walls of the loops. These samples confirm the previous results that the leaching of chromium is the only major change with either fulinak 14 or fuzrna 27. The metallic ingredients of the fuel were found to a depth of 20 mils with fulinak 14 and 6 mils with fuzrna 27. This seems to indicate that some of the holes do connect to the surface. Another type 316 stainless steel loop was operated for 500 hr with fulinak 14. This was accomplished by keeping the minimum temperature above 1500°F.

A series of loops has been operated in an attempt to circulate lead. The most important variable now seems to be the cleaning procedure used on the loops. A type 430 stainless steel loop circulated only 16½ hr, but a type 410 stainless steel loop that had been more thoroughly cleaned circulated 351 hours. One Inconel loop would not circulate at all, and another circulated only 2½ hours. All the plugs were located at the bottom of the cold leg.

Inhibitors. In the static corrosion studies, various materials are being investigated as possible inhibitors for use with molten fluorides. The most likely materials found in these tests will be tested in the thermal convection loops. One material that appeared worth trying was zirconium metal, however, its great affinity for the various gases and the difficulties in obtaining adequate mixing would make it difficult to add zirconium metal to a loop either before or after heating. Zirconium hydride was tried instead, since it decomposes slightly below operating temperatures and is stable at lower temperatures Another advantage of the hydride is that during its decomposition, nascent hydrogen is liberated, which may also have a beneficial effect.

Two Inconel loops, 225 and 242, have been operated at 1500°F with a ½% zirconium hydride addition to fulinak 14. The maximum penetration found was only 0.5 mil in the first loop and 1 mil in the second. This is the smallest amount of attack yet found in a loop circulating fluorides. Figure 17 is a hot leg section of loop 242. A material not yet identified was present in some of

TABLE 6 RESULTS OF EXPERIMENTS WITH INCONEL LOOPS OPERATED AT A HOT LEG TEMPERATURE OF 1500°F

LOOP NO	CLEANING PROCEDURE	COOLANT	TIME OF CIRCULATION (hr)	REASON FOR TERMINATION	METALLOGRAPHIC NOTES		CHEMICAL NOTES
					Hot Leg	Cold Leg	
224	Degreasing	Fulinak 14 plus NaK	500	Scheduled	Intergranular pitting up to 10 mils	Thin surface layer with some adhering nonmetallic particles	Cr increased only slightly, Fe decreased
230	Hydrogen	Fnazrk 24	500	Scheduled	Light intergranular pitting, average 4 mils, maximum 7 mils, grains not outlined	No deposited layer	Cr increased slightly, Fe decreased, others varied
226	Hydrogen	Funazrk 26	500	Scheduled	Widely scattered intergranular pitting, average 7 mils, maximum 10 mils	Both metallic and nonmetallic deposits	Cr increased, Fe and Ni de creased, others varied
229	Degreasing	Not treated, fulinak 14	500	Scheduled	Moderate to heavy intergranular pitting, up to 18 mils, average 8 mils	Thin deposit, at least partly nonmetallic	Large increase in Cr, Fe de creased, small decrease in U and F
227[a]	Degreasing	Fulinak 14	500	Scheduled	Moderate to heavy pitting, 6 to 16 mils, mainly intergranular attack	Very thin metallic layer	Cr increased, Fe decreased, U quite uniform
234	Degreasing	Fuzrna 27	480	Power failure	Light, scattered intergranular pitting, up to 5 mils, average 2 mils, dirty Inconel used	Both metallic and nonmetallic crystals on the walls	Cr increased, large decrease in Fe and Ni, increase in U
236	Hydrogen	Fuzrna 27	462	Power failure	Moderate intergranular pitting, average 8 mils, maximum 10 mils, some pits in grains	Both metallic and nonmetallic particles on wall	Cr increased, Fe and Ni decreased, U increased
225	Degreasing	Fulinak 14 plus ½% ZrH_2	500	Scheduled	Very little attack, surface rough, few pits, 0 5 mil, possibly some attached crystals, precipitate formed in crystal boundaries	Metallic layer, 0 2 mil, layer quite adherent	Cr, Fe, Ni, and U decreased
231	NaK	Fuzrna 27	500	Scheduled	Moderate general pitting, up to 9 mils	Both metallic and nonmetallic particles deposited on wall	Cr increased, Fe, Ni, and U decreased
237	Na	Fuzrna 30	500	Scheduled	Typical Inconel pitting, maximum penetration 7 mils, average 5 mils	Rough surface with nonmetallic and probably metallic crystals adhering	Cr increased, U, Zr, Fe, and Ni decreased
238	NaK	Fulinak 14	500	Scheduled	Moderate general and intergranular attack, maximum 12 mils, average 7 mils	Thin nonmetallic layer	Fe and U decreased, Cr increased slightly
223[b]	NaK	Fulinak 14	500	Scheduled	Typical Inconel attack, 8 to 10 mils, depth slightly deeper in crevice, but double amount found	Thin nonmetallic deposit	Fe and U decreased, Cr in creased
241	NaK	Fuzrna 27 plus 10 cm^3 of NaK	500	Scheduled	Light pitting and intergranular attack, maximum 4 mils, average 1 5 mils	Metallic deposit and needlelike metallic crystals	Zr and Fe decreased, U, Cr, and Ni varied
235	NaK	Fulinak 14 plus ½% Cr	455	Power failure	Typical Inconel attack, more grain boundary preference, maximum 13 mils, average 8 mils	Thin layer that penetrates into irregu larities, seems to be nonmetallic	Added Cr still in top pot, Fe and U slightly decreased
240[c]	Degreasing	Fulinak 14	500	Scheduled	Moderate attack, up to 11 mils, sample only attacked 3 mils	Thin surface deposit	
239[d]	Degreasing	Fuzrna 27	500	Scheduled	Moderate to heavy attack, 9 to 17 mils, sample only attacked 1 mil	Light, spatty deposit with some metallic crystals	
243	Degreasing	Fuzrna 27 plus ½% ZrH_2	500	Scheduled	Widely scattered attack, 1 to 4 mils	Very thin surface deposit and deposits of crystals	
242	Degreasing	Fulinak 14 plus ½% ZrH_2	500	Scheduled	Widely scattered attack, 1 mil, occasional deposits in some grain boundaries	Metallic layer with nonmetallic particles occluded	
244	Degreosing	Fuzrna 27	500	Scheduled			

[a] Hot leg annealed ½ hour – 1750°F
[b] Lap joint in hot leg
[c] Sample in hot leg
[d] Sample in top of hot leg

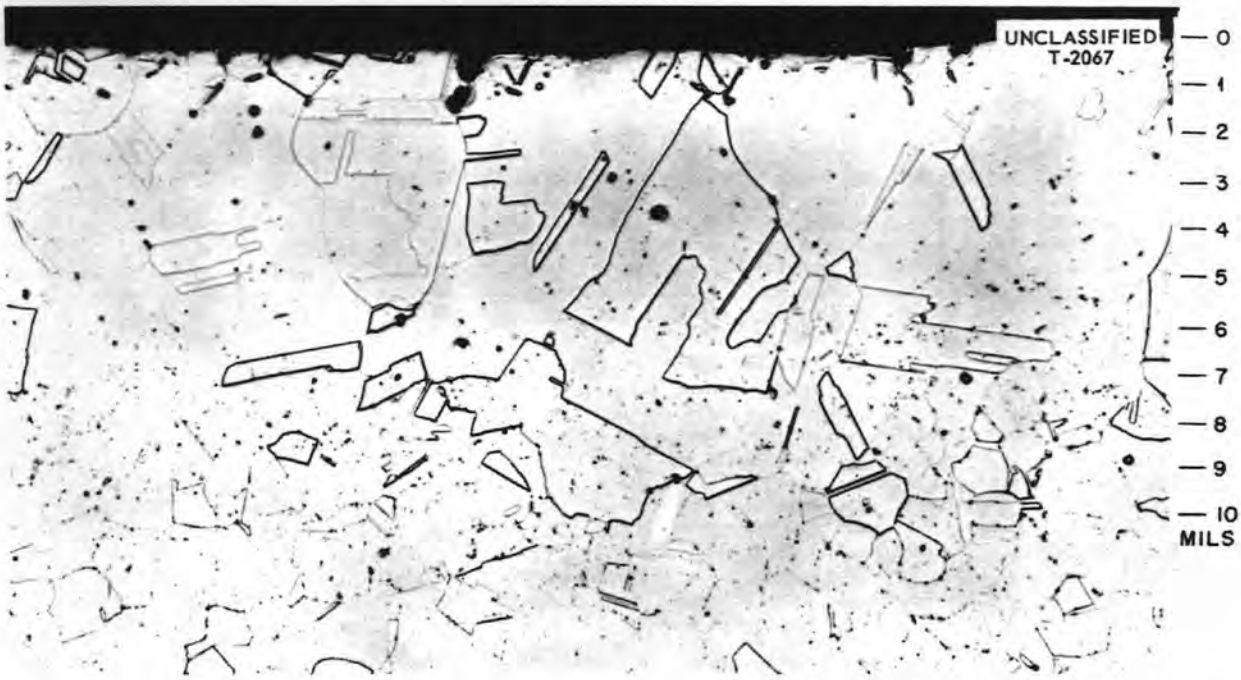

Fig. 17. Hot Leg Section of Inconel Loop 242 Operated for 500 hr at 1500°F To Circulate Fulinak 14 with ½% ZrH_2 Added. Etched with aqua regia. 250X

the grain boundaries in the hot legs of these loops, and a thin adherent layer that appears to be metallic was found in the cold leg of each loop. Reduced corrosion was additionally evidenced by the quite low amount of metallic impurities found in the fluorides after the runs. Both hot and cold leg sections have been turned over to the x-ray laboratory for diffraction studies. The coolant in these loops segregated into two phases on cooling; one is the usual green phase and the other is colorless. These two phases were present as alternating layers.

Since optimistic results were obtained with the loops discussed above, a loop was run with zirconium hydride added to fuzrna 27. In this loop the effect on corrosion was not so marked as in the others. The attack was scattered, with a maximum depth of 4 mils and an average depth of 2 mils. This represents a reduction both in depth and amount of attack, but the attack was not eliminated. No grain boundary constituent was present in this loop. A considerable change occurred in the appearance of the fuel, which now consists of alternating layers of a brownish red material and the usual green phase. The reddish brown material was identified petrographically as being made up of two phases, one of which was a slightly altered complex of zirconium fluoride and uranium fluoride.

The static corrosion studies also showed optimistic results with base metals as inhibitors. Previously reported work also showed a reduction in attack when nonuranium-bearing fluorides were circulated with NaK additions. Small amounts (~10 cm^3) of NaK were added to two Inconel loops. Loop 224 circulated fulinak 14 and loop 241 fuzrna 27. With these materials, both the amount and maximum depth of attack were lower than in comparable loops without the NaK. The improvements were not large and could have resulted from the normal spread in results. The fact that the metallic impurities in the fluorides were so low would indicate, however, that the improvements were real. With the loop in which fuzrna 27 was circulated, a change had taken place in the appearance of the fuel. A yellow material was present as clumps and as a grain boundary constituent. Purple crystals were found in the cold sump. This loop also gave considerable difficulty during start-up. The cold leg temperatures were lower than normal and continuously decreased. Several times, agita-

tion was necessary to keep the material circulating. After 24 hr, the loop appeared to be almost completely plugged, but after agitation, the cold leg temperature suddenly rose to above 250°F, and normal circulation began. This seems to indicate that when the fuzrna 27 first contacted the NaK, a crystal mass was formed. This mass was washed into the loop and became lodged at the bottom of the cold leg. It gradually dissolved or disintegrated until it suddenly broke up and circulation became normal.

Since chromium is the material being leached from the hot leg, the addition of chromium to the fuel could possibly slow down the reaction. It would be necessary to keep the chromium concentration low enough to prevent saturation and deposition in the cold leg but high enough to reduce the rate of solution in the hot leg. The solubility of chromium in the fluorides has not yet been determined. A loop was operated with a chromium addition, but the results are inconclusive since the chromium did not mix into the loop itself. Chromium powder (–325 mesh) equivalent to ½% of the fluorides was placed in the top pot and fulinak 14 added to it. The maximum hot leg attack was 13 mils, which is a normal figure. The analysis of the fluorides showed a chromium concentration in the various loop sections that was even lower than normal. The fluorides in the expansion pot were also analyzed, and over 5% chromium was present There was a thin ring around the "water line" of the pot that was found, by spectrographic means, to be primarily chromium The reason for the chromium not mixing into the loop has not been determined.

Loop Cleaning. The standard loops have been cleaned only by degreasing with a solvent degreaser. It was realized that oxide layers were not removed by such a procedure, but the oxide was felt to be more desirable than the variables introduced by pickling. Heating in a dynamic dry-hydrogen atmosphere seemed to be a possible method for reducing the oxides without attacking the metal. This operation was used on several Inconel loops in which various fluoride fuels were later circulated. When these loops were compared with similar loops that were degreased, the attack, as shown by the number of holes, was reduced However, the attack that was present was concentrated in a few boundaries and actually extended to a greater depth. In cleaning with dry hydrogen, temperatures in excess of 1850°F are necessary in some sections to provide a minimum temperature of 1750°F. These high temperatures cause grain growth and, possibly, concentration of impurities in the grain boundaries. The boundaries are then preferentially attacked.

Since hydrogen firing did reduce the amount of attack, another method of removing the oxide without causing grain growth seemed likely to give the desired results. In static corrosion studies it was found that NaK at 1500°F would remove weld scale from Inconel. Therefore several Inconel loops were cleaned by heating the hot leg to 1600°F, the cold leg to 1500°F, and circulating NaK for 4 hours. The NaK was drained while the loop was still hot. Before being operated, the loops were reheated and evacuated. Loops were run with No. 27 and No. 14 fuels and with lead. In every case the attack was as deep as that found in a degreased loop. It seems likely that when the NaK was drained, sodium or potassium oxides were left behind in the cold spots. In an Inconel loop in which lead was circulated, the loop was washed with water after being cleaned with NaK. The exit water was very basic and contained considerable caustic and confirmed the presence of the sodium and potassium. Even though NaK is not successful as a cleaner in a thermal loop, it may be useful as a cleaner in a forced-circulation loop in which a filter may be used to remove the oxides.

Crevice Corrosion. Crevice corrosion is one pessimistic aspect that must be investigated further. In an Inconel pump loop operated with flinak 12 by the Experimental Engineering Section and turned over to Metallurgy Division for examination, very little attack was found in the regular loop. However, increased attack was found in two different types of crevices. One type of crevice resulted from sleeves joining pipe sections and the other from a thermocouple well. This loop had operated for about 1000 hr at 1250°F and lower and for 100 hr at 1500°F.

The crevice corrosion effect was then checked by examining the welds in the tops of several loops. The penetration of weld metal was not complete, and by choosing the proper field, crevices could be found. In Table 7, the attack found in the crevices is compared with the attack on the walls directly opposite. Figure 18 shows a section through a joint of Inconel loop 219.

TABLE 7. CREVICE CORROSION IN THERMAL CONVECTION LOOPS

LOOP NO.	COOLANT NO.	MAXIMUM ATTACK (mils)		COMMENTS
		Hot Leg	Crevice	
219	14	3	6	Two to three times more attack in the crevice
229	14	4	6	Many times more attack in the crevice
234	27	3	5	Very little attack in hot leg with moderate amount in the crevice; tendency for attack to follow grain boundaries

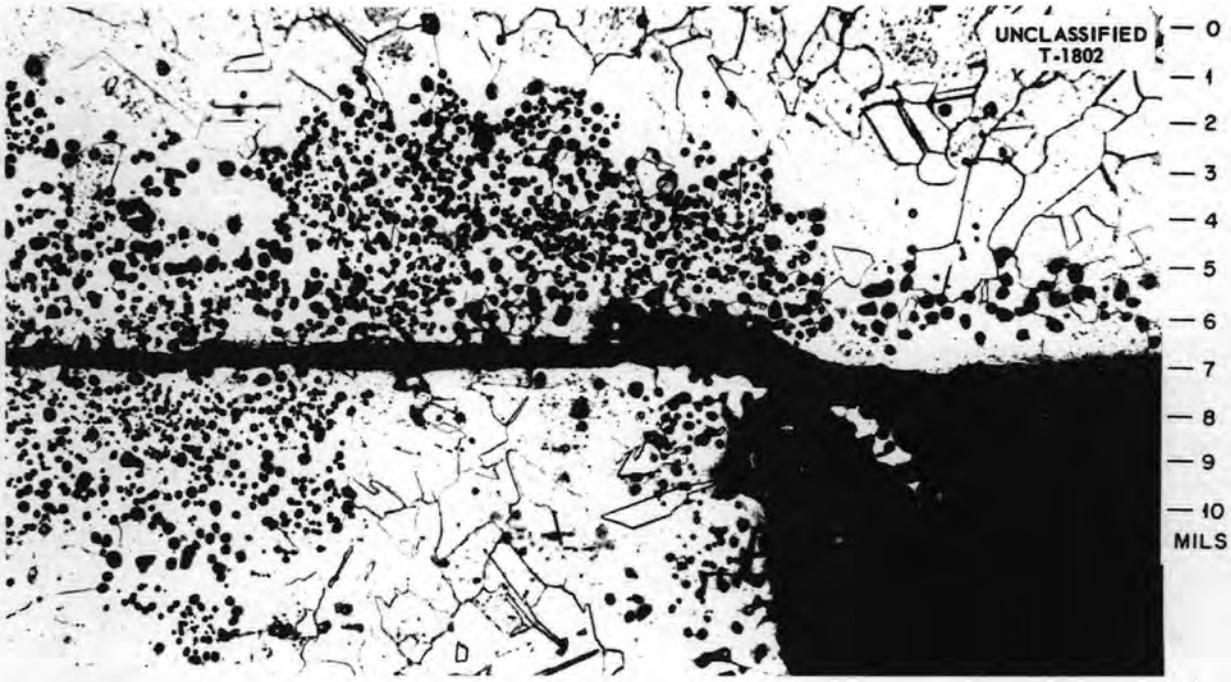

Fig. 18. Hot Leg Crevice of Inconel Loop 219 Operated for 500 hr at 1500°F To Circulate Fulinak 14. Etched with aqua regia. 250X

It should be pointed out that attack in the portions of the hot legs in which crevices were found was considerably less than that shown in Table 7. However, the crevices were in the portions above the heaters, whereas the portions usually examined are within the heaters. The decrease in corrosion is probably caused by a very slight temperature drop. Regardless of the reason for the attack being less in the upper sections, the opposite sides of the same wall should be under as nearly the same conditions as it is possible to obtain and should provide a valid comparison. Additional evidence for the existence of crevice corrosion is that there is less attack at the mouth of the crevice than within. The mechanism of this attack is not yet known, and further tests will be made to determine just how serious the effect will be.

As an additional check on this variable, an Inconel loop was fabricated with two crevices in the hot leg, and fulinak 14 was circulated in the loop at 1500°F. The wall attack in the upper section of the hot leg varied from 4 to 7 mils, whereas the attack in an adjoining crevice was from 6 to 8 mils and twice as concentrated. At the lower crevice only scattered pitting, up to 5

mils deep, was shown on the pipe, whereas normal attack, up to 6 mils, was found in the crevice. This loop showed only a slight increase in depth of attack in the crevices but a considerable increase in amount.

Change in Wall Analysis. Additional drillings have been made from the inside of the loop walls, and steps were taken to assure that the pipes were not deformed during the drilling. The chemical analyses of these samples are given in Table 8. Loop 229 is an Inconel loop in which fulinak 14 was circulated under standard conditions. A maximum attack of 18 mils and an average of 8 mils were found in the hot leg. A thin deposit was observed in the cold leg. The change of analysis with depth from the surface follows the same general pattern as that obtained for the loops discussed in the previous report. The chromium concentration of the surface was less than before, but the nickel concentration increased slightly. The Fe-to-Ni ratio remained constant from 6 mils down, which showed that the changes in nickel are in only the surface layers. The chromium, as before, was leached to a considerable depth,

TABLE 8. ANALYSES OF LOOP WALLS

DEPTH OF CUT (mils)	COMPOSITION (%)									
	Fe	Ni	Cr	Fe/Ni	NaF*	KF*	ZrF_4*	LiF*	Other**	Total
Loop 229, Hot Leg										
3	6 73	81 7	8 19	0 083	0 26	0 74		0 81	1 34	99 77
6	6 83	80 9	9 38	0 085	0 26	0 44		0 41	1 19	99 41
10	6 99	79 7	11 1	0 088	0 14	0 30		0 27	1 23	99 73
15	6 98	78 1	13 1	0 089	0 11	0 15		0 22	1 40	100 16
20	6 85	77 8	14 2	0 088	0 07	0 12		0 16	1 42	100 62
25	6 91	76 8	15 4	0 090					1 47	100 58
30	6 87	76 4	15 6	0 089					1 66	100 53
External	6 90	76 5	16 0	0 090					1 36	100 76
Loop 229, Cold Leg										
3	8 46	73 8	16 6	0 114					1 45	100 31
6	8 15	74 6	16 5	0 110					1 64	100 89
10	7 82	74 4	16 7	0 105					1 75	100 67
15	7 63	74 5	16 6	0 102					1 79	100 52
20	7 72	74 4	16 5	0 104					1.64	100.26
External	7.62	74 6	16 7	0 102					1 65	100 57
Loop 236, Hot Leg										
3	11 7	74 8	10 3	0 156	0 14		0 92		1 61	99 47
6	9 44	74 6	13 7	0 126	0 04		0 55		1 49	99 82
10	9 02	74 8	14 8	0 121					1 75	100 37
15	7 70	74 4	16 5	0 103					1 56	100 16
20	7 70	74 1	16 6	0 104					1 43	99 83
25	7 63	74 3	16 5	0 102					1 56	99 99
30	7 68	74 2	16 6	0 103					1 56	100 04
External	7 68	74 6	16 6	0 103					1 35	100 23

* Values calculated from spectrographic analysis of the metals, by assuming that they were present as fluorides

**Total of Ca, Cu, Si, Al, Mg, Mn, and Ti from spectrographic analysis

since even in the 25 to 30 mil cut, the chromium concentration was not so much as at the surface. One difference in these analyses is that the metallic ingredients in the fuel (sodium, potassium, and lithium) were found, spectrographically, only to a depth of 20 mils. In previous samples they were still present at 30 mils. Since the pipes are not perfectly round after operation and the original samples were deformed in drilling, the dimensions are only approximate. The deformation during drilling may account for the apparent depth of the fuel in the original test. Although most of the holes do not connect to the surface, some of them must connect to allow the fuel to be present at 20 mils. In the cold leg of this loop no base metals were found at any level. The chromium and nickel concentrations remained unchanged, but the iron in the surface layer had been increased by 1%. However, the iron content gradually decreased to a normal value at a depth of 10 mils.

For comparison, the hot leg of Inconel loop 236 was drilled. The fuzrna 27 that had been circulated in this loop produced a hot leg attack that averaged 8 mils, with a maximum of 10 mils. The chromium concentration was reduced, but not so much as in loop 229, and returned to normal at 10 mils. The iron concentration of the surface increased considerably but was normal at 10 mils. The iron impurity in the original fuel was much higher than normal, so this increase in iron may not be a normal occurrence. The nickel remained essentially unchanged. The metallic constituents of the fuel (sodium and zirconium) extended only to a depth of 6 mils.

Miscellaneous Loops. A type 316 stainless steel loop has operated 500 hr, circulating fulinak 14, with no sign of plugging. This loop operated with a minimum cold leg temperature of 1510°F and a corresponding hot leg temperature of 1630°F and is only the second stainless steel loop to circulate fluorides for 500 hours. This and the other loop operated under similar conditions. The first successful loop, 123, has been examined, and intergranular attack of 13 mils was measured in the hot leg. A metallic layer 1 mil thick (much thicker than usual) was found in the cold leg. The temperatures in the second loop were turned back to normal (1500°F) at 500 hr, and the loop has circulated for an additional 100 hours. Plugging now seems to be gradually taking place.

The Izett iron loop, which had been cleaned with dry hydrogen, plugged in 46 hr with fulinak 14 at 1500°F. The inside surface of the hot leg was very rough, and considerable reduction in wall thickness had taken place. A heavy metallic deposit in the form of large metallic crystals with some nonmetallic particles embedded in them was found in the cold leg.

Self-insulating Properties of Fluorides. An Inconel loop was filled with fulinak 14 and allowed to circulate in a normal manner at 1500°F. After normal circulation was established, two helium jets, each of which delivered over 1000 cfh, were directed against an area at the top of the cold leg. They did not cause plugging in 18 hours. The cold leg temperatures dropped initially, but the power was gradually increased and the temperatures returned almost to normal. The helium jets were then replaced by air jets with 80-psi pressure from ¼-in. tubing. In the area where the air strikes the loop, a black spot about 6 in. long is present, but loop operation is unaffected. This loop has now circulated over 1000 hr with the air jets in place, and apparently there has been no plugging.

Dynamic Testing of Lead. Work on the problem of circulating lead has been resumed this quarter. Loops identical to those being used with the fluorides are being employed in this work. The lead used in the tests is chemical lead, which has been further purified by bubbling hydrogen through it.

Lead was first circulated in two Inconel loops. The first loop, which had been cleaned with NaK (cf., section on "Loop Cleaning"), would not circulate lead at all. The second loop was rinsed with water before being evacuated and then cleaned with NaK. The wash water leaving the loop contained considerable caustic. This loop circulated only 2½ hours. The lowest cold leg temperature, recorded just before complete plugging took place, was 1170°F. The cold leg was heated with the resistance heater to over 1350°F, but circulation could not be restarted. The lead was drained from both loops, and plugs were found in the lower portions of the cold legs. These plugs would not melt at 1575°F. Besides the plugs, a mass resembling a vine and occupying about one-fourth the volume was found wound around the inside of the cold leg in each loop. These masses held their shape where they turned into the hot legs. Analyses of these masses show them to be high in nickel and lead, however, the x-ray diffraction lines do not fit those from any material in the system

A type 430 stainless steel loop was rinsed with cold nitric acid, washed with water, and then evacuated while hot. This loop circulated lead for 16.5 hours. The two cleaning methods were then combined and used on a type 410 stainless steel loop. This loop was cleaned with NaK, washed with water, rinsed with cold nitric acid, washed again with water, and heated while under vacuum. It circulated lead for 351 hr at 1500°F before plugging. Plugs that were left in both loops when the lead was melted out at 1575°F again appeared to be at the bottom of the cold leg. The plugs have been submitted for chemical and x-ray diffraction study.

STATIC CORROSION

D. C. Vreeland E. E. Hoffman
L. D. Dyer

Fluoride Corrosion. In previous static corrosion tests in Inconel tubes with fluoride 14 plus sodium metal additions of approximately 1%, there was little or no attack on the Inconel. Similar tests with much lower additions of sodium (approximately 0.17%) have now been completed on both Inconel and type 304 stainless steel, and no attack could be noted. These tests were for 100 hours at 816°C.

Copper was also tested in fluoride 14 for 100 hr at 816°C. This test is of interest because some of the brazing alloys being considered for ARE application contain copper. No dimensional changes could be noted after test, and metallographic examination revealed no attack.

AGOT graphite was tested in fluoride 14 for 100 hr at 816°C. A graphite capsule was used to contain the specimen and the molten salt. A visual examination of the specimen after test revealed no erosion or other attack, no dimensional changes were noted. There was a slight weight loss, 0.0078 g/sq in.

Tests were run in Inconel tubes for 100 hr at 816°C with fluoride 14, plus approximately 10% additions of ferric oxide, nickel oxide, and chromic oxide to determine whether such oxides, which may also be present on Inconel, would increase the corrosion by fluorides. The nickel oxide and ferric oxide had little or no effect on the extent of corrosion, and the addition of chromic oxide apparently increased corrosion. The results are summarized in Table 9.

In some tests run with fluoride 14 for 100 hr at 816°C, sections of the testing tube were taken both above and below the bath level. Corrosive attack could be noted on all sections examined. This would seem to indicate that attack can be expected on metals exposed to the vapor phase of the fluoride mixtures. The sections of type 304 stainless steel exposed to the vapor phase appeared to be attacked more severely than those exposed to the liquid phase. Inconel and types 309 and 316 stainless steels appeared to be attacked by the vapor phase to approximately the same extent as by the liquid phase of the molten fluoride salts. Figures 19 and 20 compare specimens of type 304 stainless steel exposed to the liquid phase and to the vapor phase of the fluoride. Details of these tests are presented in Table 10.

Hydroxide Corrosion. A survey of the abstracts contained in ORNL-1291[1] indicated that additions of CaO, $Ca(OH)_2$, $NaNO_2$, $NaNO_3$, and $NaClO_3$ might have some effect in inhibiting corrosion by hydroxides. CaO and $Ca(OH)_2$ were reported to participate in reactions of the following type

$$Na_2CO_3 + Ca(OH)_2 \longrightarrow 2NaOH + CaCO_3,$$

$$Na_2CO_3 + CaO + H_2O \longrightarrow NaOH + 3CaCO_3.$$

Reactions for the alkali metal nitrites and nitrates

[1] M Lee, *General Information Concerning Hydroxides*, ORNL-1291 (April 21, 1952)

TABLE 9. RESULTS OF CORROSION TESTS OF INCONEL IN FLUORIDE 14 WITH CERTAIN ADDITIVES FOR 100 hr AT 816°C

ADDITION	METALLOGRAPHIC NOTES
10% ferric oxide	Attack to 2 mils on specimen and tube
10% nickel oxide	Attack to 1 mil on specimen and tube
10% chromic oxide	Attack to 5 mils on specimen and 2 to 10 mils on tube

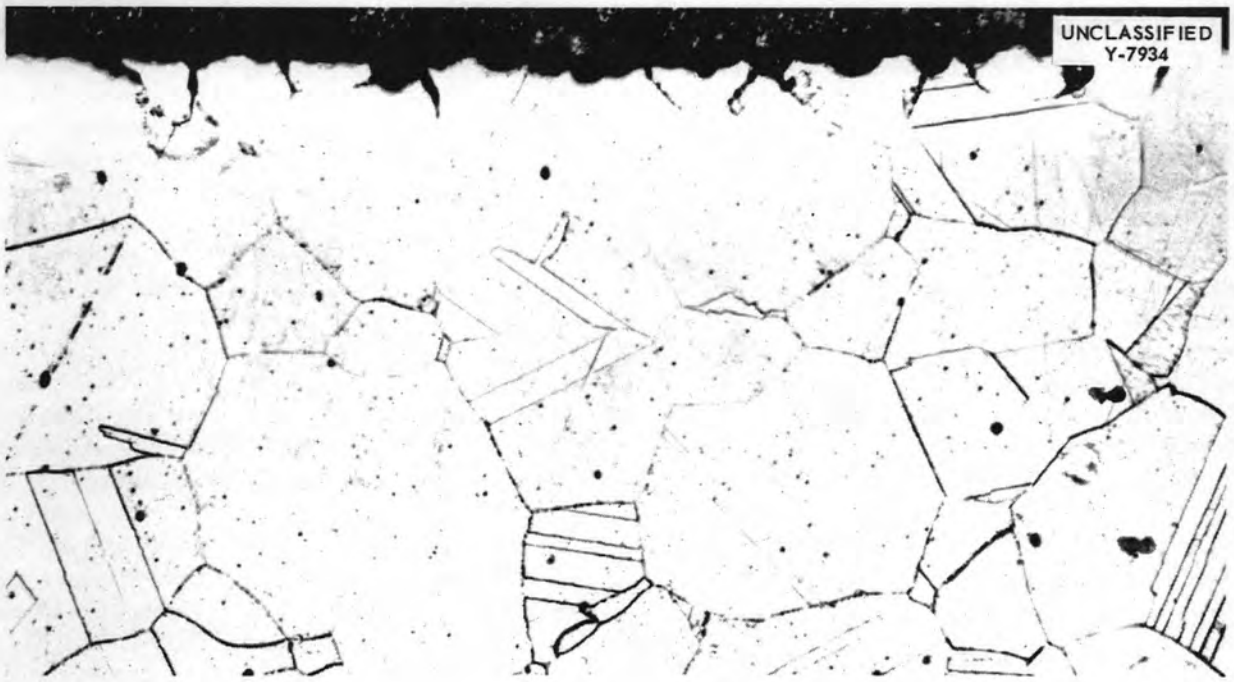

Fig. 19. Type 304 Stainless Steel Exposed to Liquid Phase of Fluoride 14 for 100 hr at 816°C. Etched with aqua regia. 250X

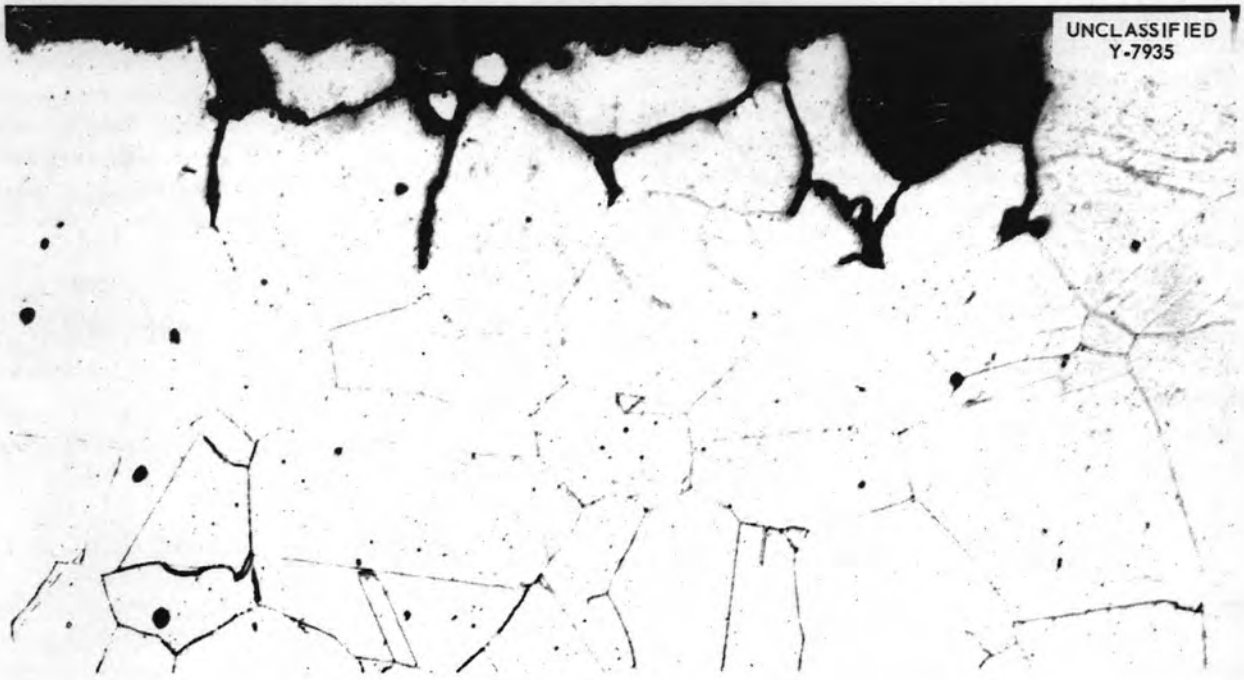

Fig. 20. Type 304 Stainless Steel Exposed to Vapor Phase of Fluoride 14 for 100 hr at 816°C. Etched with aqua regia. 250X

TABLE 10. RESULTS OF EXAMINATIONS OF VARIOUS MATERIALS EXPOSED TO LIQUID AND VAPOR PHASES OF FLUORIDE 14 FOR 100 hr AT 816°C

MATERIAL	METALLOGRAPHIC NOTES	
	Liquid-Phase Exposure	Vapor-Phase Exposure
Inconel	Erratic attack, subsurface voids to 1.5 mils	Erratic attack, subsurface voids to 1 mil
Type 304 stainless steel	Erratic attack, intergranular attack with some subsurface voids to 1 mil	Intergranular attack to 5 mils
Type 309 stainless steel	Subsurface voids to 3 mils	Subsurface voids to 3 mils
Type 316 stainless steel	Intergranular penetration, 1 mil	Some slight evidence of attack, less than 0 5-mil penetration

TABLE 11 RESULTS OF STATIC TESTS OF TYPE 316 STAINLESS STEEL IN SODIUM HYDROXIDE WITH VARIOUS ADDITIVES FOR 100 hr at 816°C

ADDITIVE	METALLOGRAPHIC NOTES
5% $NaClO_3$	Unattacked material decreased from 33 to 26 mils
5% $NaNO_2$	Unattacked material decreased from 33 to 25 mils
5% $NaNO_3$	Unattacked material decreased from 33.5 to 20 mils, intergranular penetration beneath uniform corrosion layer, 1 to 2 mils
5% CaO	Unattacked material decreased from 33.5 to 26 mils
5% $Ca(OH)_2$	Unattacked material decreased from 33.5 to 26 mils

and sodium chlorate were not given, but the reduction of corrosion by these additives was stated to be as much as 90% under certain conditions. Static tests were run with type 316 stainless steel exposed to sodium hydroxide at 816°C for 100 hr, approximately 5% additions of the above-mentioned additives were made to the sodium hydroxide. None of these additives seemed to have any effect in inhibiting corrosion. It is believed that the inhibiting effect mentioned in the literature[1] may take place at much lower temperatures than were employed in these tests. The test results are presented in Table 11.

A series of tests was completed on the effect of temperature on the corrosion resistance of types 304 and 316 stainless steels in sodium hydroxide (100 hours). Attack on these materials was not noticeable until the test temperature was increased to at least 550°C. The results are tabulated in Table 12.

Static tests in sodium hydroxide of an 80% Ni–20% Mo alloy and an 80% Ni–20% Fe alloy were run for 100 hr at 816°C. The 80% Ni–20% Mo alloy showed subsurface voids to a depth of 1 to 2 mils, and the 80% Ni–20% Fe alloy showed subsurface voids to a depth of 3 to 5 mils upon metallographic examination.

A test was run of beryllium oxide in potassium hydroxide contained in an Inconel tube with a hydrogen atmosphere. The hydrogen was purified with a deoxo unit. The potassium hydroxide was dehydrated under vacuum for 56 hr, by gradually raising the temperature to 500°C before the beryllium oxide specimen was introduced. During the test a constant flow of hydrogen through the system was maintained. The period of the test was 100

TABLE 12. RESULTS OF TEMPERATURE-DEPENDENCE TESTS IN SODIUM HYDROXIDE FOR 100 HOURS

TYPE OF STAINLESS STEEL	TEMPERATURE (°C)	METALLOGRAPHIC NOTES
304	350	No attack
304	450	No attack
304	550	Light intergranular penetration, 0 5 to 1 mil
304	650	Unattacked material decreased from 34 to 24 mils
316	350	No attack
316	450	No attack
316	550	Intergranular attack, 1 to 2 mils

hr and the temperature was 800°C. The beryllium oxide was rather severely attacked. Weight and dimensional changes are listed below.

	Before Test	After Test
Length, in.	0 486	0.413
Width, in	0.263	0.207
Thickness, in	0.269	0.213
Weight, g	1.5254	0.6882

Metallographic examination of the Inconel tube used in this test revealed a 4- to 10-mil oxide layer.

Liquid Metals. A dynamic test, which has become known as the spinner test, has been used to check the effect of high velocities on corrosion and erosion of several materials in molten sodium. In this test tubular specimens are rotated at relatively high velocities (400 ft/min) in a pot containing the molten corrodant under isothermal conditions. Inconel and types 316, 347, and 446 stainless steels have been tested in this apparatus. Greater attack than in ordinary static corrosion tests was noted on all materials tested. It should be emphasized that inasmuch as the spinner pot was fabricated of type 347 stainless steel, these were actually three-component tests, except in the case of the type 347 stainless steel specimens. The attack on Inconel after spinning at 400 ft/min at 816°C for 72 hr is shown in Fig. 21. A 0.5-mil surface layer and 0.5 mil of intergranular voids beneath it are apparent. This surface layer may be a mass transfer effect caused by the three-component system used during test. An analysis of a portion of the surface layer scraped from the specimens showed 64% Ni, 27.5% Cr, and 8.3% Fe. The composition of Inconel is generally accepted as 80% Ni, 15% Cr, and 5% Fe.

Figure 22 shows the intergranular attack on type 316 stainless steel tested for 100 hr at 816°C with a speed of 400 ft/min. The attack extended to a depth of 1 to 2 mils near the front or leading edge of the tubular specimen and, as would be expected, was less severe at the trailing edge, where the depth of attack was 0.5 to 1 mil. Type 347 stainless steel suffered intergranular attack to 2 mils after 74 hr at 816°C and a speed of 400 ft/min. The attack on this material is shown in Fig. 23.

Type 446 stainless steel showed slight intergranular attack, to a depth of less than 0.5 mil, after 53 hr at 816°C at a speed of 400 ft/min. The results of these tests are summarized in Table 13.

A series of static corrosion tests of various ceramic materials received from the Ceramic Laboratory has been tested in sodium at 816°C for 100 hr in Inconel tubing. The results are tabulated in Table 14. Only two of the specimens were intact after test Al_2O_3 and spinel. Many of the specimens disintegrated into a fine powder during the test, other specimens were broken into several pieces. It is possible that if these specimens had been thicker (specimens were approximately 20 mils thick), some of them might not have broken up during the test.

PHYSICAL CHEMISTRY OF CORROSION

G. P. Smith J. V. Cathcart
W. H. Bridges

Inhibition of Mass Transfer. Previous studies of mass transfer made with a small thermal convection loop indicated that a hydrogen gas atmosphere had

TABLE 13. RESULTS OF SPINNER TESTS RUN AT 400 ft/min AT 816°C

MATERIAL	TIME OF TEST (hr)	METALLOGRAPHIC NOTES
Inconel	72	Surface layer attack to depth of 0.5 mil with 0.5 mil of intergranular voids beneath
Type 316 stainless steel	100	Intergranular attack, 1 to 2 mils deep on leading edge and 0.5 to 1 mil deep on trailing edge
Type 347 stainless steel	74	Intergranular attack, up to 2 mils
Type 446 stainless steel	53	Slight intergranular attack, less than 0.5 mil

TABLE 14. RESULTS OF TESTS OF VARIOUS CERAMIC MATERIALS IN SODIUM FOR 100 hr AT 816°C

MATERIALS	OBSERVATIONS AFTER TEST
Porcelain (Al-576)	Disintegrated during test
Mica	Disintegrated during test
Titanium dioxide (Al-192)	Disintegrated during test
SiO_2	Disintegrated during test
Barium titanate (Al T 106)	Disintegrated during test
Al_2O_3 (single crystal)	Disintegrated during test
Lead glass	Disintegrated during test
ZrO_2 (Hf-free)	Disintegrated during test
ThO_2	Disintegrated during test
$2MgO\ SiO_2$ (Fosterite, Al 243)	Disintegrated during test
$2MgO\ 2Al_2O_3 \cdot 5SiO_2$	Disintegrated during test
Aluminum silicate (Al A)	Disintegrated during test
Pyrex glass	Disintegrated during test
Zirconium silicate (Al 475)	Disintegrated during test
HfO_2	Disintegrated during test
Soda glass	Disintegrated during test
TAM ZrO_2	Disintegrated during test
$MgO \cdot SiO_2$	Disintegrated during test
Al_2O_3	Increase in thickness, 3 mils, weight increase of 0.01 g/in.^{2}
SiC	Specimen broken into several pieces, no thickness change
MgO	Specimen broken into several pieces, no thickness change
MgO (single crystal)	Specimen broken into several pieces, no thickness change
Spinel	No change in thickness, weight loss of 0.006 g/in.^{2}
ZrO_2 (Al 550)	Specimen shattered, 1 mil increase in thickness
Zircon	Specimen shattered, 1.5 mil increase in thickness
BeO	Specimen shattered, 7 mils increase in thickness

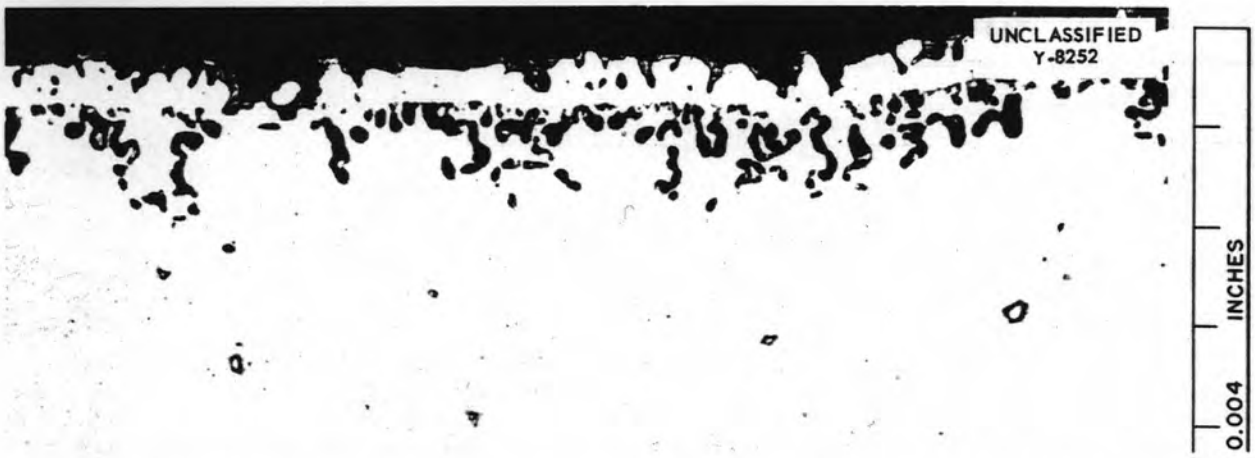

Fig. 21. Inconel from 400-ft/min Spinner Test at 816°C for 72 Hours. Note surface layer.

Fig. 22. Type 316 Stainless Steel from 400-ft/min Spinner Test at 816°C for 100 Hours. 250X

Fig. 23. Type 347 Stainless Steel from 400-ft/min Spinner Test at 816°C for 74 Hours. 250X

an appreciable effect in reducing nickel mass transfer. This effect has been more closely investigated with special apparatus, and although the research is by no means complete, encouraging results have been obtained. Molten sodium hydroxide was contained in a nickel cup into which was immersed a nickel tube with a closed end. Thermocouples were attached to the outside of the nickel cup and to the inside of the nickel tube. These parts were enclosed in a quartz vessel with a pyrex stopper. The temperature of the nickel cup was maintained by a furnace that surrounded the quartz vessel. The temperature of the inner nickel tube could be separately controlled at a temperature lower than that of the nickel cup by means of a strong current of air that flowed to the bottom of the nickel tube and then passed out through a small pyrex tube. In this manner a controlled temperature difference could be maintained between the nickel cup and the inner nickel tube.

In the experiments the sodium hydroxide was dehydrated in the apparatus under vacuum by slowly raising the temperature to 500°C over a period of several days. Tests showed that no appreciable mass transfer occurred during this dehydration. Then the desired atmosphere was admitted to the apparatus, the temperature of the nickel cup was raised to operating temperature, and the air stream was turned on to cool the inner nickel tube.

The results of two typical tests are illustrative of the results of the several experiments made. In both tests the temperature of the nickel cup was about 725°C, whereas the temperature of the inner nickel tube was 525°C, a temperature difference of 200 degrees. The first test was conducted with a static vacuum over the hydroxide melt. In 40 hr, a copious quantity of dendritic nickel crystals had encrusted the inner nickel tube and extended more than half way across the hydroxide melt. This is a case of the normally expected nickel mass transfer in sodium hydroxide for a large temperature difference.

In the second test a purified hydrogen atmosphere replaced the static vacuum. In 170 hr, as compared with 40 hr for the first test, the only evidence of mass transfer obtained was a tiny band of nickel crystals on the inner nickel tube at the gas-liquid interface. This band was about 1 mm wide and 0.1 mm thick.

Confirmatory evidence for the inhibiting effect of hydrogen has been obtained with the tilting furnace apparatus designed by Brasunas.[2] Richardson of the Metallurgy Division modified this test so that the hydroxide melt could be maintained under hydrogen at a pressure of 1 atm and conducted a single test. In this test, when the liquid was in the heated end of the furnace it was at a temperature of about 725°C, and when in the cold end it was at 650°C, a difference of 75 degrees. The cycling rate was about 4 tilts per minute.

In order to keep the pressure at 1 atm, it was necessary to add hydrogen continuously. The hydrogen loss is believed to have been due to diffusion through the walls of the hot Inconel tube. A slowly decreasing rate of diffusion was observed, which was probably the result of the gradual thickening of the oxide film on the outside of the Inconel tube.

After 100 hr of operation no evidence of mass transfer was obtained. Of about 75 tests with the tilting furnace, this is the only nickel-sodium hydroxide test in which mass transfer did not occur. The other tests were under a variety of conditions but without a hydrogen atmosphere.

These tests show that hydrogen has a marked effect in inhibiting the mass transfer of nickel in molten sodium hydroxide under simple test conditions.

New Tripositive Nickel Compounds. Two new tripositive compounds of nickel have been identified as corrosion products of nickel attacked by sodium hydroxide in the presence of oxygen gas. The purpose of this investigation was twofold. First, in corrosion and mass transfer studies with the hydroxides, a variety of black and colored products has been obtained that do not correspond to any known nickel compounds. The occurrence of these products has caused some difficulty in the efforts to ascertain the mechanism of hydroxide corrosion. Therefore an effort to identify some of the more unusual corrosion products and determine some of their physical and chemical properties was

[2] Figure 35, *ANP Quar Prog Rep March 10, 1952*, ORNL-1227, p. 121.

desirable as an aid in future identification and in determination of how they might have been formed.

The second purpose of this investigation was to determine whether nickel ions of valence greater than 2 might occur in hydroxide melts. These higher valence ions are required by the very ingenious mechanism of nickel mass transfer proposed by Grimes of ORNL and Hill of Duke University about a year ago. At that time the only nickel compounds of valence greater than 2 for which there was any but the most tenuous evidence were four trivalent nickel oxyhydroxides and a hydrous oxide of quadravalent nickel.

The most important features of the work done thus far are briefly summarized here. Two compounds, with the empirical formulas $NaNiO_2$ and $LiNiO_2$, have been prepared. These compounds, which will be called sodium nickelate(III) and lithium nickelate(III), have been identified by chemical analysis for nickel and for the alkali metals, by several chemical reactions, including a quantitative determination of oxidizing power and a reaction that gives a known trivalent nickel compound, and by complete crystal structure analysis.

Sodium nickelate(III) was prepared in a simple apparatus, which consisted of a 1-in. A nickel tube 12 in. long that had been crimped and welded closed on one end. Sodium hydroxide (c.p.) was melted in the tube, and a ½-in. nickel tube, the end of which had been crimped but not welded, was immersed in the hydroxide melt. Oxygen gas was passed through this tube at a rate of about 3 ml/sec and allowed to bubble through the melt.

The hydroxide was heated in the temperature range of 650 to 850°C for 48 hours. Then the ½-in. inside tube was removed from the melt, and the 1-in. tube containing the molten hydroxide was quenched in oil and quickly stoppered. The removal of the inner nickel tube and the contraction of the hydroxide on freezing caused the liquid level to drop considerably and leave exposed a heavy encrustation of black crystals attached to the tube wall. Examination of several tubes revealed that although there was a quantity of black crystals distributed throughout the frozen hydroxide, the greatest concentration occurred in the heavy deposit at what had been the gas-liquid interface. Next, the nickel tube was cut and the end of the tube containing the black crystal deposit was squeezed in a vise. The crystals thus loosened were stored in a desiccator over Dehydrite. These operations were carried out as rapidly as possible. Finally, the crystals were washed with absolute ethyl alcohol, to remove adhering sodium hydroxide, and vacuum dried.

It will be noted that in the above procedure the bulk of the hydroxide had separated from the crystal deposit before the washing with alcohol. This gave a saving in time that was important, since it was found that leaching the black crystals out of the solid hydroxide with absolute alcohol took considerable time, during which time part of the trivalent nickel present was reduced to divalent nickel. The alcohol became a deep red and a quantity of resinous deposit was produced. This reaction was probably the result of an aldol condensation.

Four batches of black crystals were analyzed for sodium, nickel, carbon, and the ratio of trivalent nickel to total nickel present. The results of these analyses are given in Table 15. The analyses are in good agreement with the calculated analysis for sodium nickelate(III).

TABLE 15. ANALYSES OF BLACK CRYSTALS

BATCH	COMPOSITION (%)				Ni^{+++}-TO-Ni RATIO
	Sodium	Nickel	Oxygen	Carbon	
A	21.3	51.0	27.7*	0.13	
B	20.7	51.3	28.0*		1.00
C	20.4	50.9	28.7*		
D	20 7	51.6	27.7*		1.00
Calculated for $NaNiO_2$	20.2	51.6	28.2		1.00

*Calculated by difference

The analysis for trivalent nickel was performed by digesting the compound in a hydrochloric acid solution of potassium iodide under an inert atmosphere. The iodine liberated by the reduction of Ni^{+++} to Ni^{++} was titrated with standard thiosulfate.

To obtain single-crystal x-ray patterns, a binocular microscope was mounted in a dry box with the eye pieces of the microscope waxed to the outside of the dry-box window to facilitate observation. A preparation of $NaNiO_2$ was removed from the furnace and while still hot was placed in the dry box. After the $NaNiO_2$ cooled, some crystals were scraped out of the nickel tube and placed under the microscope, where a specimen was selected and sealed in a glass capillary. These precautions were found to be necessary in handling the tiny x-ray specimens because of their reactivity with the moisture in the air and with the stopcock grease and the other organic materials that had been used in an effort to coat them.

Structure analysis showed the unit cell of $NaNiO_2$ to be monoclinic with dimensions a = 5.328 Å, b = 2.858 Å, c = 5.588 Å, and β = 110°30′. There are two molecules, per unit cell, whose atoms have the following positions

2 Ni	000, ½½0
2 Na	0½½, ½0½
4 O	$\pm(U0z)$, $\pm(U+½,½,z)$

where U = 0.220 and z = 0.700. Figure 24 is an electron density map of a unit cell of this compound.

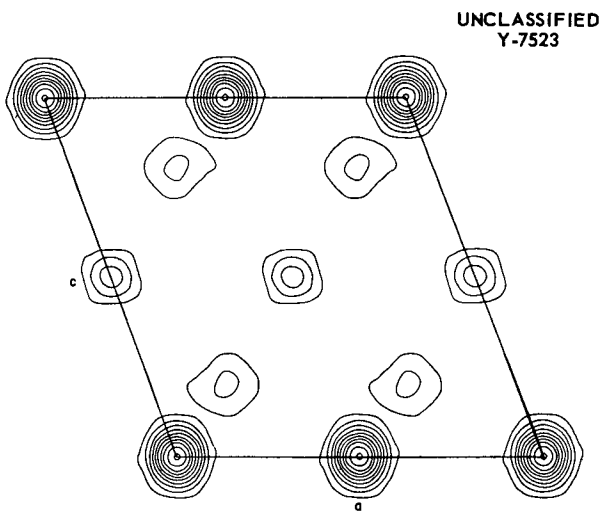

Fig. 24. Fourier Projection of $NaNiO_2$ on (010).

A powder pattern was obtained for an alcohol-washed sample. The small crystallites tended to arrange themselves with a preferred orientation, so the observed line intensities were of no use for structure determinations, but the line positions showed that the alcohol washing had not affected the $NaNiO_2$ structure.

The reaction of $NaNiO_2$ with water was given some attention because of the frequent practice in corrosion tests of removing excess hydroxide with a water wash. One sample of alcohol-washed $NaNiO_2$ was divided into two parts sample M was washed with water several times, and the washings did not turn phenolphthalein pink, sample N was washed continuously for two weeks. The following tabulation gives the results of analyses for sodium and nickel in samples M and N and the calculated analyses for sodium and nickel in $NaNiO_2$ and NiOOH

	Na (wt %)	Ni (wt %)
Sample M	1 55	1 0
Sample N	58 0	58 4
NiOOH (calc)	0	64 0
$NaNiO_2$ (calc)	23 2	51 6

Analysis for Ni^{+++} showed that the ratio of Ni^{+++} to total nickel was between 0.5 and 1, but this particular Ni^{+++} determination cannot be specified any closer.

Sample M was examined by x-ray diffraction techniques, and two types of crystals were observed. One was a distorted $Ni(OH)_2$ lattice, the other corresponded to a rhombohedral cell that, if assumed to be the oxyhydroxide NiO(OH), gave a structure almost identical to that reported for γ-NiO(OH) by Glemser and Einerhand.[3]

A 2-g sample of $NaNiO_2$ was placed in 100 ml of refluxing water for 11 days, and an x-ray powder pattern of the product was obtained that did not correspond to any known nickel compound.

A preliminary microscopic examination of $NaNiO_2$ crystals revealed some distinctive properties. When the crystals were immersed in a drop of water, the properties progressively changed to those characteristic of γ-NiO(OH). During this water reaction the crystal did not crumble or otherwise lose its form. X-ray measurements have been made on a crystal of $NaNiO_2$ while it was decomposing into

[3] O. Glemser and J Einerhand, *Z anorg Chem* 261, 26-51 (1950).

γ-NiO(OH). Progressive changes in the single-crystal patterns were observed but have not been analyzed.

A second method for preparing $NaNiO_2$ was used in which 25% Na_2O_2 instead of bubbling oxygen gas was added to the fused caustic. The compound thus prepared appeared to be the same as that obtained with oxygen gas.

$LiNiO_2$ was prepared by a technique similar to that used for $NaNiO_2$. The reaction, however, was much more rapid, and thin-walled nickel tubes were completely disintegrated in less than 24 hours. Thick nickel pipe was found to be satisfactory for holding the melt, but the tube through which oxygen was introduced invariably disintegrated before the end of a run. The product was a very fine, tightly compacted, crystalline powder in contrast to the large $NaNiO_2$ platelets. It was found that a mass of powder frequently contained particles of unreacted nickel metal that could be removed with a magnet after the lump of product had been crushed. It was difficult to remove the adhering lithium hydroxide by alcohol washing, and no samples were obtained that were entirely free of the hydroxide. An analysis was made of a sample that had been washed with considerable alcohol, and the results are given in Table 16. It may be seen that the lithium content is higher and the nickel content lower than those calculated for pure $LiNiO_2$. However, if it is assumed that the excess lithium is present as lithium hydroxide (1.815%), the nickel content is brought more nearly in line with the theoretical value, as shown by the corrected analysis also given in Table 16. The analysis for Ni^{+++} shows that all the nickel present is in the Ni^{+++} form, to within experimental error.

Samples of the black powder that had not been alcohol washed were prepared for x-ray examination with a flat sample holder by a dry-box technique similar to that used for handling $NaNiO_2$ samples. A spectrometer trace was taken, and the pattern was successfully indexed by assuming the structure to be rhombohedral and of the $CsICl_2$ type. The rhombohedral cell dimensions are a = 5.013 Å and α = 33°22 . There is one molecule per unit cell, with atoms in the following positions

Ni	000
Li	½½½
O	$\pm(UUU)$

where U = ¼. The cell dimensions, referred to hexagonal axes, a' = 2.878 Å and c' = 14.19 Å, contain three molecules and the calculated density is 4.8 g/cm^3. The measured density is 4.8 g/cm^3. The atoms lie in the following positions of space group C^2_{3i} (or D^7_3, or D^5_{3d})

$(000, \frac{1}{3}\frac{2}{3}\frac{1}{3}, \frac{2}{3}\frac{1}{3}\frac{2}{3})+$

Ni, 3a	000
Li, 3b	00½
O, 6c	$00z, 00\bar{z}$.

An oxygen parameter of z = 0.25 gave good agreement between observed and calculated intensities, as shown in Table 17. Also compared in this table are observed and calculated values of $\sin^2 \theta$.

A sample of $LiNiO_2$ was washed with running water for eight days. Chemical analysis showed 5.55% Li, 62.4% Ni, and a decrease in the Ni^{+++}-to-Ni ratio. The x-ray pattern for this material was the same as that obtained for undecomposed $NaNiO_2$.

The known compound $NaFeO_2$ was successfully prepared by techniques similar to those described for alkali nickelates(III). It was hoped that possibly some hexavalent iron would be formed, but no evidence for this was found.

It is interesting to compare the structures of $LiNiO_2$ and $NaNiO_2$ with those of similar materials. In $LiNiO_2$ the oxygens are almost perfectly cubic closed-packed. If the packing were perfect, c'/a' would be $2\sqrt{6}$ or 4.90, and α of the rhombohedral

TABLE 16. ANALYSES OF $LiNiO_2$

	COMPOSITION (%)			Ni^{+++}-TO-Ni RATIO
	Lithium	Nickel	Sodium	
Original analysis	8 48	54 9	0 062	1 00
Corrected analysis	7 11	58 5		1 00
Calculated for $LiNiO_2$	7 11	60 1	0	1 00

TABLE 17. OBSERVED AND CALCULATED INTENSITIES AND $\sin^2\theta$ FOR $LiNiO_2$

hkl	OBSERVED INTENSITY	CALCULATED INTENSITY	OBSERVED $\sin^2\theta$	CALCULATED $\sin^2\theta$
003	160	170	0 0266	0 0265
011	66	84	0 0986	0.0986
006	16	10	0 1062	0.1062
102	23	29	0 1073	0 1074
014	151	135	0 1428	0.1428
105	25	34	0 1693	0.1694
009		6		0 2389
017	28	19	0 2401	0 2401
108	42	38	0 2843	0 2844
110	41	38	0 2868	0 2868
113	21	24	0 3132	0 3134
201	9	8	0 3855	0 3854
01,10		5		0 3906
116	15	9	0.3926	0 3930
022		3		0 3942
00,12	7	6	0.4249	0 4248
204	17	18	0 4292	0 4296
10,11	12	6	0 4529	0 4525
025		6		0 4561
119	12	11	0.5262	0 5258
207		5		0 5269
028	12	13	0 5706	0.5712
01,13		5		0.5941

cell would be 33°34′. The observed values are $c'/a' = 4.93$ and $\alpha = 33°22'$. The small nickel and lithium cations lie in alternate layers in the octohedral interstices of the oxygen array. Each cation has six oxygen neighbors, and each oxygen has three lithium and three nickel neighbors. Most of the other compounds of the $CsICl_2$ type are similar to $LiNiO_2$, but not so closely packed. For example, the rhombohedral angle for $NaFeO_2$ is 30°20′, and for $NaCrS_2$ it is 29°48′.

The lattice of $NaNiO_2$, on the other hand, is of a more complicated type in which there are moderate deviations from what would have been expected for the closest packing of ions.

Calculation of the crystal radii for the ions in $LiNiO_2$ and $NaNiO_2$ gives 1.42 Å for O^{--}, 0.6 Å for Li^+, 0.9 to 1.0 Å for Na^+, and 0.6 Å for Ni^{+++}. Values given by Pauling[4] are 1.40 Å for O^{--}, 0.60 Å for Li^+, and 0.95 Å for Na^+. This represents good agreement. No previous values are available for Ni^{+++}, but the value for Fe^{+++} is 0.60 Å.

Consideration of the data obtained on the action of water on the alkali nickelates(III) shows this to be an interesting complex reaction. The γ-NiO(OH) obtained from the reaction of $NaNiO_2$ with

[4] L. Pauling, *Nature of the Chemical Bond*, p. 350, Cornell Univ Press, Ithaca, N. Y., 1945.

water has an unusual crystal structure that, even though related to the structures of AlO(OH) and FeO(OH), involves some unexpectedly large interatomic spacings that have not been satisfactorily explained. The occurrence of $Ni(OH)_2$ in the preparation of γ-NiO(OH) is not unlike a substance that Glemser and Einerhand reported to consist of NiO(OH) irregularly embedded between normally developed $Ni(OH)_2$ layers. In this latter substance, however, the NiO(OH) does not correspond in lattice dimensions to α-, β-, or γ-NiO(OH). The reaction of $NaNiO_2$ with hot water apparently yields another new compound of nickel. The results of the x-ray examination of the product obtained from the reaction of $LiNiO_2$ with water are puzzling in that the original material and the product gave the same pattern. This may have a trivial explanation – the observed lines may have come only from unreacted $LiNiO_2$, since there was appreciable lithium in the product. However, there is also the possibility that the NiO(OH) was formed in which hydrogen ions were substituted in the positions that had been occupied by lithium ions. This would be a new crystal modification of NiO(OH), but this substance is already known to occur in at least four modifications at room temperature. The difficulty encountered in removing the alkali metal from $LiNiO_2$ and from $NaNiO_2$ by washing with water, even for long periods of time, is interesting. This may be due in part to an association between the OH^- of the alkali hydroxide with the OH^- of the oxyhydroxide to give strong sorption. It would be difficult, however, to account in this manner for the large quantity of Li^+ ions retained.

The various aspects of the reaction of the alkali nickelates(III) with water are of some practical interest, since they emphasize the difficulty to be encountered in analyzing the data obtained with water-washed corrosion specimens.

In summary, the work performed on the chemistry of corrosion products in the sodium hydroxide-nickel system has been the determination of new trivalent nickel compounds, together with a study of some of their reactions.

Mass Transfer in Liquid Lead. Studies are being made of the mass transfer of molybdenum and of Inconel in liquid lead. Research has been conducted on the handling and purification of liquid lead, and a few mass transfer measurements have been made.

Initially, measurements were desired on the mass transfer of molybdenum in liquid lead at temperatures up to 1000°C. However, these measurements presented some problems in apparatus design. The construction and operation of conventional thermal convection loops constructed largely of molybdenum is not feasible because molybdenum metal is expensive and difficult to weld. Furthermore, it oxidizes excessively at high temperatures, and such a thermal convection loop would have to be operated under an inert-atmosphere blanket that would have to be cooled to take care of heat removal from the cold leg of the loop. Therefore it was decided to perform the experiments in apparatus made of quartz or pyrex, depending on the temperature to be used, since these materials are resistant to corrosion by liquid lead[5] and do not present the problem of the three-component system that would be encountered if the apparatus were made of a metal other than molybdenum.

Studies were made of the deoxidation of high-purity lead. From the quantity of oxide that collected on the surface of lead melted under purified hydrogen, it was concluded that the original material had contained considerable occluded oxide. A number of experiments was performed in which hydrogen was passed in fine bubbles formed by a fritted pyrex disk through molten lead at 450 to 500°C for 20 hr, and the lead was then filtered through a fritted pyrex disk. There were no visible oxide films on the surface of the filtered lead, but a small amount of oxide was found on the filter. This indicated that the hydrogen reduction had not been complete. Further studies of the conditions required for complete reduction by hydrogen will be made.

An experiment was performed to determine whether molybdenum mass transfers during temperature cycling in the manner reported[6] for copper in bismuth. A mechanically polished molybdenum specimen was contained in lead, and the temperature was cycled for 42 hr between 500 and 510°C with a cycle time of 12 minutes. At the end of the cycling, the lead was filtered at 500°C. No mass transferred crystals were found. This result should be taken as preliminary, because the molybdenum was undoubtedly coated with an oxide film that may have prevented contact with the molten lead.

[5] R. N. Lyon (ed), *Liquid Metals Handbook*, p. 105, NAVEXOS P-733 (June 1, 1950)

[6] G. P Smith and J. V Cathcart, *Met Quar Prog Rep Jan 31, 1952*, ORNL-1267, p 85

It had been planned that other mass transfer measurements would be made with molybdenum, however, it was decided that measurements of the mass transfer of Inconel in liquid lead were needed, and hence the molybdenum studies were discontinued.

The studies of the mass transfer of Inconel in liquid lead have been initiated with quartz loops, not because Inconel loops would not be satisfactory, but in order to hasten the development of techniques for operating loops made of fragile quartz. The initial loop design is shown in Fig. 25. The loop was made of quartz tubing containing two sections of Inconel tubing. The lead purification flask was made of pyrex glass and was joined to the quartz loop by means of a water-cooled standard-taper joint. Pyrex was used because quartz fritted disks were not available. All parts of the system were heated, except the water-cooled joint.

The proposed method of operation was to deoxidize the lead in the 300-ml bulb at 500°C by bubbling hydrogen up through the fritted disk, evacuating the loop, and forcing the molten lead through the filter and into the loop under hydrogen pressure. Two loops have been set up. The first loop broke during heating because the holders that clamped the loop in place were not properly designed. This was corrected for the second loop, but an unexpected freeze-up of the lead occurred when it was being transferred from the deoxidation flask to the heated loop. A second type of loop has been designed in which the standard-taper joint has been eliminated. This loop requires a satisfactory quartz fritted disk, which is being developed in the ORNL Glass Shop.

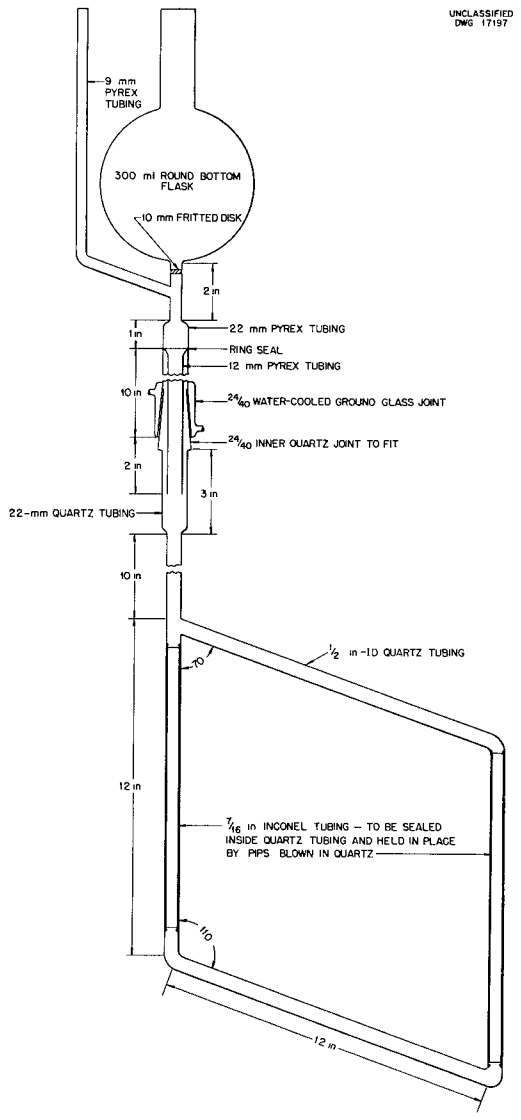

Fig. 25. Apparatus for Measuring Mass Transfer of Inconel in Liquid Lead.

CERAMICS RESEARCH

J. M. Warde
C. E. Curtis
L. M. Doney
S. D. Fulkerson
J. R. Johnson
A. J. Taylor
G. D. White

CERAMIC COATINGS FOR METALS

Radiator Coatings (ANP). Further work was carried out on the application of a ceramic coating to nickel for possible use in a radiator. It was found that by annealing specimens of pyrometallurgical nickel 10 mils thick in an atmosphere of wet hydrogen for 65 hr at 1000°C, sufficient carbon can be removed to permit good adherence of NBS coating A-418, applied at 1700°F. The coated specimens showed only 0.05% weight gain in a 9-day oxidation test at 1500°F. Work is under way to apply coating A-418 to a nickel radiator assembly.

Coatings with High Boron Content. At the suggestion of E. P. Blizard of the Physics Division, work was started on developing a ceramic coating containing a minimum of 10% boron and a method of applying the coating to metals. A preliminary composition was developed that was satisfactorily flame-sprayed onto 20-gage stainless steel. In order to carry out tests on the shielding properties of this coating, it will be necessary to place it on a 5-ft-square mild steel plate $\frac{7}{8}$ in. thick. This operation is beyond the capacity of the flame-spray equipment in the Ceramic Laboratory, and the Ohio State Engineering Experiment Station, which has more suitable facilities, was requested to make further attempts. This Station reports that the coating has been successfully applied to a $\frac{5}{8}$-in.-thick mild steel plate in a preliminary test. Arrangements will be made to coat the 5-ft-square test plate.

CERMET INVESTIGATION

The study of ceramic and metal combinations (cermets) continues. In order to decide on the most suitable compositions for investigation, the following elements and combinations, which have very low neutron-absorption cross sections and which meet other reactor design requirements, were studied

Be	Be_2C	BeO	MgO
Si	SiC	SiO_2	Al_2O_3
Zr	ZrC	ZrO_2	CaO

Two materials (Si and SiC) are listed that have been successfully combined commercially to make a refractory, oxidation-resistant material. It is planned to attempt the development of fuel elements by combining Si, C, and U_2C, and a small vacuum-induction furnace has been designed for firing the specimens. It is suggested that such fuel elements might be satisfactory for unshielded, guided-missile reactors (direct cycle) and possibly a helium-cooled, stationary, power reactor.

The hydrogen cleaning system developed for use with the cermet firing equipment has proved satisfactory, and several 70% chromium–30% Al_2O_3 bars have been successfully fired. This composition has been studied in some detail by other investigators, and because of its familiarity, was selected as a starting material to check the operation of the equipment available. Several disks, 1 in. in diameter and 24 mils thick, were pressed with this composition, as well as two "sandwich" uranium oxide-containing specimens, these materials have been successfully fired and are being studied.

A number of ZrC-Fe cermet specimens were made by T. S. Shevlin at the Ohio State Experiment Station and have been submitted to the Metallurgy Laboratory for tests in fluorides and NaK. This cermet has been found to have relatively poor oxidation resistance.

HAFNIUM CARBIDE INVESTIGATION

Synthesis of Hafnium Carbide. After several trials with 20-g samples of HfO_2 + C, a procedure has been developed that gives a fairly consistent product containing HfC and HfN in varying proportions. In this procedure HfO_2 powder (–300 mesh) is mixed with carbon (atomic graphite, 2.5 μ), in stoichiometric proportion, to give hafnium carbide. This powder mixture is then cold pressed at 10,000 psi to form a pellet $\frac{3}{4}$ in. in diameter and about $\frac{1}{2}$ in. long. The pellet is then placed in a graphite crucible, which, in turn, is placed in a larger crucible fitted with a sight tube. The whole assembly is then heated by induction to about 2000°C in 45 minutes. During the next hour,

the temperature is raised to 2400°C. The temperature is then increased to above 3000°C for 10 min, after which, the crucible is allowed to cool to room temperature. A black crystalline mass results.

The method described in patent No. 2,124,509 for producing hafnium carbide has also been tried. In this method, HfO_2 is placed in molten aluminum metal with excess carbon present and the mixture is heated to above 2000°C. The results look promising.

Fabrication. About 200 g of hafnium carbide, prepared by the pellet process, has been sintered and ground, acid treated, washed, and dried. A cold pressed bar has been made and will be sintered at 2100°C. This specimen will be used for thermal expansion tests and other investigations.

Hardness. One sample of hafnium carbide had large crystals and hence was ideal for the determination of hardness by the Vickers method. The average of four Vickers determinations made by the Metallography group was 2910.

Refractoriness. A small piece of hafnium carbide has been heated to above 2500°C in the small phase furnace in an argon atmosphere. A reaction with the tungsten filament took place at above 2600°C, however, a sample of hafnium carbide was held at 2440°C in contact with the tungsten filament, with no visible reaction and no melting. There is some evidence that the vapor pressure (or dissociation pressure) of hafnium carbide becomes significant in the vicinity of 2500°C.

X-Ray Analysis. The presence of hafnium carbide in three samples has been established by Steele and Bredig of the Chemistry Division. They also found HfN and carbon.

Chemical Analysis. Several samples were analyzed for nitrogen, carbon, and hafnium, all the samples contained combined nitrogen and free carbon. The best composition from the standpoint of lack of free carbon was

	Actual (%)	Theoretical (%)
Hafnium	92 4	93 7
Carbon	2 35	6 3
Nitrogen	3 84	

Since this compound was produced in an argon atmosphere, the presence of the nitrogen is difficult to understand.

ANP REACTOR DESIGN – CERAMIC REFLECTOR

An efficient and economical material is required for use as a reflector-moderator for a liquid-cycle aircraft reactor, and it was suggested that a glass-bonded beryllium oxide material be considered. The material should have nearly zero porosity and should contain a minimum of 60 mole % beryllium oxide. The glass forming the bond should also contain a small amount of beryllium oxide, consistent with viscosity requirements for fabrication. Simulated mixes of soda-lime-silica glasses and silica sand were fabricated on a small scale, and it was found that such a material could successfully be prepared. There were small air bubbles in the initial lots prepared, but these could be eliminated by suitable techniques.

Such a reflector could be cooled by sodium flowing in metal pipes embedded in the glass-bonded beryllium oxide. Once the glass-bonded beryllium oxide had been poured into the shell and had flowed around the cooling pipes, it would be necessary that the temperature of the reactor shell be maintained just above the annealing range of the glass bond.

A sample of glass-bonded beryllium oxide was prepared by the Ceramic Laboratory, and IBM calculations for the efficiency of this material were completed. The results are tabulated in the following, along with results for other materials for comparison

Moderator	Critical Mass (relative units)	Relative Neutron Leakage
Be	10	0 00029
BeO	10	0 0025
BeO (aggregate)	~35	0 0104
Graphite (ρ = 1 87)	42	0 040
NaOD	~60	0 0023
D_2O	8	0 000092

The matrix composition was 75 mole % BeO and 25 mole % glass bond. The composition of the glass was Na_2O 0.25 BeO 2.5 SiO_2, the density was 2.61. The above tabulation indicates that for the "Fireball Reactor" design the proposed beryllium oxide-glass mixture is somewhat better than the best obtainable graphite (1.87 density), although it is not so good as beryllium metal or beryllium oxide.

Further studies will be made of this material. The devitrification tendencies of the glassy matrix

and the corrosion effect of the glass on stainless steel or other cooling-pipe materials will be determined. It is felt that although this material is not so satisfactory as beryllium metal for an aircraft reactor, it offers promise as an economical moderator, and it is suggested that consideration be given to it as the moderator-reflector for reactors for ships, submarines, terrestrial power, etc., in which shield weight is not so critical as in aircraft.

SLURRY FROM MAGNESIA CRUCIBLES

At the request of the Engineering Department, an investigation was carried out on the production of a slurry from used magnesia crucibles that can be pumped. The investigation showed that the crucibles should first be sized to a minimum of $\frac{1}{8}$ in. and then ball-milled with 30 to 40% water (based on the total weight of the slurry). Approximately 1% (of the dry weight of the MgO) of aluminum nitrate should be added to retard settling. Agitation is desirable if the suspension is allowed to stand over 1 hour. If the slurry is not processed for periods of 6 hr or more, water should be added from time to time to replace that which reacts with MgO.

HIGH-TEMPERATURE X-RAY STUDIES OF THORIUM AND HAFNIUM OXIDE

Several high-temperature x-ray photographs of thorium and hafnium oxide were made. The thorium films indicated no phase changes at 1500°C but suggested a possible cubic-lattice growth phenomenon similar to that observed with cerium at low temperatures. Further work is in progress.

According to the film obtained, hafnium oxide remains monoclinic up to about 1600°C, but some change occurs between 1600 and 1900°C. Further work has been delayed because of the softening of the cement holding the beryllium windows in the camera. The investigations will continue as soon as the windows are replaced. A series of tests was made to determine the true black-body temperatures of the hafnium oxide specimens at the point of x-ray beam contact. Similar tests will be made on thorium.

HRP METALLURGY

E. C. Miller

WELDING AND FABRICATION SPECIFICATIONS FOR STAINLESS STEEL AND PRESSURE VESSEL STEELS

W. J. Leonard

The experimental work in welding various materials is incidental to the preparation of procurement and procedural specifications adapted to the requirements of the HRP and to the facilities available in the Laboratory and in the Y-12 shops. Welded plates of 1-in.-thick type 347 stainless steel have been sectioned and are being studied by metallographic methods. These sections contain welds of various filler rod stainless steels, including type 347. Also, 1-in. plates of stainless steel (type 347 and type AISI 1025 carbon steel) were welded with type 347 stainless steel rod and with a modified type 307 stainless steel rod and sectioned for metallographic examination. At present, 2-in. plates of type 347 stainless steel are being prepared for welding tests.

SURFACE HARDENING OF TITANIUM FOR VALVE TRIM

A. R. Olsen T. W. Fulton

Efforts are continuing toward the development of a suitable nitrided case on titanium valve parts required by the HRE and engineering design groups. Suitable surface hardness is obtained by heating in a purified nitrogen atmosphere. The coating is brittle, however, and must be kept thin to avoid chipping. This, in turn, makes it difficult to finish the parts to obtain a leak-proof closure. Six surface-hardened plugs are now being tested for corrosion resistance in uranyl sulfate at 250°C. Additional work will be done with harder alloys of titanium as a base for the case. Other proposed

methods of surface hardening, including a carbonitriding process, will be tried.

TITANIUM PARTS FOR PUMPS

E. S. Bomar A. R. Olsen
T. W. Fulton

Two model 100-A pump impellers have been fabricated from RC-70 titanium, and one has been operated successfully for a short time in a loop test. Because the carbon content of the material was somewhat above that generally considered acceptable for welding, both plug welds and titanium rivets were used to fasten the two parts of each impeller.

The Y-12 shops have successfully machined a thermal spacer and pump casing from RC-70 titanium. The inlet and outlet pipes on the casing have been welded in a dry box to produce radiographically sound welds.

COOPERATION WITH HRP CORROSION GROUP

E. C. Miller A. R. Olsen
T. W. Fulton

In addition to the routine preparation and examination of specimens for the HRP static and dynamic testing groups, special metallurgical examinations and treatments are being made on components exhibiting unusual behavior in corrosive environments. Each examination or treatment usually requires the planning of additional corrosion tests to verify and further explore tentative explanations. One study involves the severe attack directly beneath a type 347 stainless steel band that held the two parts of a type 304 stainless steel sample holder together. The sample holder had been exposed to UO_2SO_4 solution containing 100 g of uranium per liter at 100°C in a dynamic loop system for 1123 hours. The attack made the metal more or less spongy and appears to be a form of crevice corrosion resulting from oxygen depletion of the solution trapped between the band and the holder. Samples taken from the holder are being subjected to various heat treatments and metallographic examination to determine whether possible sensitization of the stainless steel may have played a part in the attack. Titanium (Ti-75) sample holders apparently resist attack under comparable conditions, although they show some severe localized tarnishing, which may be the beginning of attack, and some attack in spots that is apparently related to inclusions in the metal and not to the location of the bands. A limited amount of work is being undertaken to determine the effects of prior history – thermal, mechanical, and chemical – of austenitic stainless steels on the quantity, composition, and character of the corrosion films that result from exposure to various corrosive environments.

PHYSICAL METALLURGY OF TITANIUM

W. J. Fretague

Impact tests have been carried out on specimens prepared from swaged and vacuum-annealed Ti-75A material. In addition to tests on untreated specimens, the impact tests were carried out on various specimens subjected to the following treatments to determine whether, under the conditions of test, sufficient hydrogen would be taken up to influence the impact values or transition temperatures

1. exposure in loop A (dynamic) to UO_2SO_4 solution containing 300 g of uranium per liter and pressurized with oxygen at 250°C for 100 hr,
2. cathodic treatment in 1 M H_2SO_4 at 0.1 amp for 8 hr at 70°F,
3. same as treatment 2, but for 168 hr,
4. exposure in static bomb test to UO_2SO_4 solution containing 40 g of uranium per liter and pressurized with hydrogen and oxygen (750 psi at room temperature) for ten days at 250°C (pressurized every two days).

Additional samples are being prepared for exposure in loops and in static in-pile tests, as well as for miscellaneous metallurgical preparations. Impact specimens of iodide titanium have also been prepared by d-c arc melting in argon, followed by swaging and vacuum annealing.

In considering the results obtained with commercial titanium, it appears that the various treatments to which the specimens were subjected in an attempt to load them with hydrogen in aqueous media at temperatures up to 250°C had little or no effect on the transition temperature as compared with untreated titanium tested at the same temperatures. This observation is based on limited data and should be considered as tentative until results are available from specimens exposed for much longer periods.

Iodide titanium behaved in a very ductile manner, even at temperatures slightly above the temperature

of liquid nitrogen. No transition temperature was found for iodide titanium that was vacuum annealed at 500°C. In fact, the impact energies recorded for specimens from two separate melts of iodide titanium, when tested at 196°C (liquid nitrogen boiling point), were in the same range as those obtained above the transition temperature on commercial titanium Ti-75A. Concerning the shape of the impact curves for iodide titanium, quite a bit of the impact energy recorded by the testing machine was absorbed in bending the specimen. As the testing temperature was raised slightly above room temperature (50°C), the iodide titanium specimens were so ductile that they bent (without breaking completely) far enough to permit the striking hammer of the impact pendulum to slide over the specimen. For this reason, all points above 20°C on the curves for iodide titanium should be disregarded as quantitative values.

Work is progressing on a modified Sievert's apparatus to prepare titanium-hydrogen alloy specimens by heating the specimens in a purified hydrogen atmosphere. This equipment will be employed to prepare alloys of both commercial and iodide titanium with hydrogen.

RESEARCH FABRICATION LABORATORY

J. E. Cunningham

PRODUCTION OF MTR FUEL AND AND CONTROL ROD ELEMENTS

J. H. Erwin, J. N. Hix, H. J. Wallace, G. E. Cooley, G Goldston, R. G. Cardwell, E. R. Turnbill, W. W. Proaps

Production of enriched uranium fuel and control rod elements was maintained during the past quarter at an all-time high. Besides completion of the sixth and seventh reactor loadings, three new loadings of "sweetened" elements (168 g of U^{235} per unit) were fabricated according to specifications and forwarded to Arco. A reactor loading for the three by nine rectangular MTR lattice consists of 23 fuel and 4 control rod elements. Work on the eleventh loading is 90% complete and on the twelfth loading 60% complete.

A conventional metal slitter has been purchased and placed into operation to further improve the process for production of these fuel units. The multicut slitter will be used to prepare the narrow, thin-gage strip of aluminum-silicon brazing alloy previously cut manually on a foot-operated shear. In a test of a proposed drying-in-vacuum technique, the time for the flux-drying operation was reduced from approximately 3 hr to less than 45 minutes.

Inventory results on the third and fifth batches of 7.5 kg of enriched uranium metal processed show percentage gains of 0.09 and 0.14, respectively, whereas the fourth batch showed a loss of 0.07. These over-all balances are drawn only after all the uranium contained in the samples, dross, crucibles, etc., is recovered and placed back into production channels.

MTR FABRICATION STUDIES

H. J. Wallace, J. N. Hix

Experimental work has been initiated in an effort to modify the present MTR fuel and control rod elements for improved operational performance. The studies are necessary for two reasons (1) actual operational experience shows a deficiency in $\Delta k/k$ of approximately 6% of that of the calculated design value, and (2) the heavier-than-anticipated load of in-pile experiments demand additional reactivity.

Brazing-Flux Poisoning Experiments. Two experiments were conducted to determine the amount of flux entrapped during brazing and the extent to which its presence would poison the reactor. A full-sized, dummy, aluminum fuel assembly was fabricated according to standard manufacturing techniques and carefully dissolved, the resulting solution was then analyzed for the total lithium content. Analytical results by the flame-photometer method showed that the assembly contained 1.26 g of lithium. Eutector-190 brazing flux contains approximately 30 wt % lithium plus chlorine. If this is assumed to be a typical unit, the lithium present would reduce $\Delta k/k$ by a factor of 2.7% in the MTR lattice.

To further check the poisoning effect, a critical experiment was performed in the Bulk Shielding Reactor on an MTR fuel assembly before and after brazing. The fuel plates used were taken directly from the MTR production line. The element was fastened initially by spot welding both the side plates and combs to the outermost fuel-bearing plates This procedure left the inner plates loose, but their motion was limited to several thousandths of an inch by the fixed combs and side plates. To adapt the unit for test, a BSR end box was attached to the lower end by the usual plug-welding-technique.

Since no calibration rod was available for the Bulk Shielding Reactor, it was decided to measure the poisoning effect of the entrapped brazing flux by comparing it with the poisoning effect of gold foil. The reactor was set up with the standard fuel elements and was found to go critical with all shim rods removed and the regulating rod at position of 15.2 in., or almost all the way out. When one of the standard elements was replaced with the MTR test element, the regulating rod position for criticality was found to be 8.7 inches. The test element was then removed and gold foil attached uniformly to the four sides of the element. The element was reinserted and a new critical position found. This procedure was repeated four times, and in each case approximately 11 g more of gold foil was added. Table 18 gives the data taken at each step.

The test unit was then disassembled, cleaned, and reassembled by brazing. Care was exercised during each operation to prevent damage and make certain that the plates were assembled in the same order as in the original assembly.

After brazing, the test element was again placed in the Bulk Shielding Reactor and a new critical position found. In the few days that elapsed between the initial experiment and final test, the reactor had not been taken above $\frac{1}{2}$ watt in power and none of the elements had been changed, however, it was noted that the critical position of the reactor, with all standard elements in, was 0.2 in. higher than in the previous experiment, as indicated in Table 18. By applying this correction to the reading obtained with the MTR element, it is seen from a plot of the data that the brazing added poison to the element equivalent to 30.8 g of gold. If it is assumed that this much poison is added to all elements for an MTR three by nine rectangular lattice, the poison would be equivalent to $30.8 \times 27 = 831.6$ g of gold, or a loss in $\Delta k/k$ of more than 3%.

Although the agreement between the two experiments is fair, it should be pointed out that the second test takes into account not only lithium but also chlorine and the other relatively high

TABLE 18. CRITICALITY TEST DATA ON AN MTR FUEL ELEMENT BEFORE AND AFTER BRAZING

DATA ON UNBRAZED ELEMENT	
Zero position of regulating rod	0 4 in
Rod position for criticality with standard BSR elements	15.2 in.
Rod position for criticality with unbrazed MTR element	8.7 in
Rod position for criticality with unbrazed MTR element plus 11 11 g of gold	10 7 in
Rod position for criticality with unbrazed MTR element plus 22.36 g of gold	12.5 in
Rod position for criticality with unbrazed MTR element plus 33 49 g of gold	14 1 in
Rod position for criticality with unbrazed MTR element plus 44 60 g of gold	15 7 in.
DATA ON BRAZED ELEMENT	
Zero position of regulating rod	0.4 in.
Rod position for criticality with standard BSR elements	15.4 in.
Rod position for criticality with brazed MTR element	13.9 in.
True rod position with brazed element	13 9 − 0.2 = 13.7 in.

neutron-absorption ingredients contained in the flux. Brazing studies are now in progress on new bromide and fluoride-base fluxes that contain a minimum of lithium.

Another approach to the problem is to minimize the amount of flux entrapped originally by adjustments in the brazing cycle. A full-sized dummy unit was brazed at a slightly higher temperature for a somewhat shorter time. After the dummy was dissolved, analytical results revealed that the amount of lithium contained was reduced by a factor of 2, or to 0.57 gram. More work along these lines is in progress.

Design Changes to Adjust V_{H_2O}-to-V_{Al} Ratio. Design changes in the thickness of the side plates and aluminum cladding on the active plates have been analyzed in an effort to reduce the V_{H_2O}-to-V_{Al} ratio to less than 0.60. Pertinent data on possible changes in the present MTR fuel element are given in Table 19.

Full-size dummy units of the first and third alterations were constructed, and no fabrication difficulties were encountered. In fact, it is felt that any one of the three alterations could be made and put into production within a reasonable changeover period. A dummy unit of the second alteration was not constructed, because the fabrication facilities are being fully utilized on other work.

Because of the added plate in the third alteration, the mechanical stability of the unit appears to be about the same as that of the present standard element. The gain in uranium content per assembly that resulted from this added plate is attractive.

As a final check on the performance of the new units, enriched uranium fuel elements for the first and third alterations have been constructed and will be placed in service in the LITR.

FABRICATION OF REPLACEMENT ELEMENTS FOR LITR

Nine replacement fuel elements and two control rod elements were fabricated and delivered for service in the LITR. A special active unit with nine plates and a 1- by 3-in. cross-sectional chamber running the entire length of the fuel was prepared for PSI. The unit will be used in the LITR to obtain a high virgin flux for exposure of solid-state experimental samples.

MISCELLANEOUS FABRICATION WORK

J. H. Erwin W. A. McNeish
D. E. Rosson J. B. Flynn
L. A. Amburn

As in the past, the Metallurgy Division continues, on a small scale, the fabrication of metal products for outside installations and other AEC-sponsored activities. These products vary greatly in nature, and because of the small quantity requested, they usually require custom-type construction. The major fabrication jobs completed during the quarter are described in the following

1. Fifty grams of highly enriched uranium (93% U^{235}) was rolled to a uniform 3-mil thickness and cut into strips 3 by 0.5 cm in area (minimum) for the University of California Radiation Laboratory.

TABLE 19. DATA ON POSSIBLE DESIGN CHANGES TO LOWER THE V_{H_2O}-TO-V_{Al} RATIO FOR MTR FUEL ELEMENTS

	NUMBER OF PLATES	CLAD-CORE-CLAD THICKNESS (mils)	SIDE PLATE THICKNESS (in)	WATER GAP (mils)	V_{Al}-TO-V_{H_2O} RATIO	k_{eff}	k_∞
Standard element	18	20-20-20	0 188	117	0 72	1 266	1 687
First alteration	18	20-20-20	0 125	117	0 65	1 278	1 683
Second alteration	18	15-20-15	0 125	127	0 54	1 300	1 679
Third alteration	19	15-20-15	0 125	118	0 56	1.297	1 680

2. One depleted (about 10 ppm U^{235}) uranium disk, 1.960 in. in diameter by 9 to 10 mils in thickness, was prepared for the Knolls Atomic Power Laboratory.

3. Depleted and enriched uranium strips for punching ¾-in.-dia disks, with the following specifications, were prepared for the Brookhaven National Laboratory

Material Description	Thickness (mils)	Area (in^2)
U^{238} (99 98%)	6 5 to 10	20
U^{235} (70 to 100%)	6 to 7	4
U^{235} (70 to 100%)	12 to 13	4
U^{238} (1 02%)	8 to 10	20

4. Ten grams of highly depleted uranium (0.006% U^{235}), 3 mils in thickness and 1 to 2 cm on a side, was prepared for Canada in connection with the Technical Cooperation Program.

5. One thousand normal uranium-aluminum alloy *J* slugs of 7.5% uranium content were produced for dissolving studies by the Chemical Technology Division.

6. One enriched (93% U^{235}) and one depleted (0.006% U^{235}) uranium metal disk, 1 in. in diameter and 6 to 5 mils in thickness, was prepared for the Van de Graaff generator studies at ORNL.

7. Two kilograms of normal uranium-aluminum alloy pellets containing 11 wt % uranium was prepared from extruded ¼-in.-dia bar for North American Aviation, Inc.

URANIUM FUEL PLATE PROGRAM FOR DuPONT

J. E. Cunningham R. J. Beaver
G. R. Caskey

A cooperative program has been initiated at ORNL to give technical assistance to Du Pont on their long-range fuel plate development project. The purpose of the work is to evaluate the suitability of uranium metal plate, produced by the best-known techniques, for service in future reactors at SRO.

The fabrication phase of the program consists, essentially, of preparing 12 cast uranium ingots. Eight of the ingots are to be hot rolled within a closely controlled temperature range and finished under four different conditions, namely, hot rolled, hot rolled and beta heat treated, hot rolled and cold reduced 4½%, and hot rolled, beta treated, and cold reduced 4½%. This work is approximately 90% complete.

Melting and Casting. Twelve castings have been prepared. Reactor-grade uranium was melted in magnesia crucibles and poured into graphite molds by tilting the crucible. All operations were conducted under vacuum with a pressure of less than 200 μ and, in most cases, at a pressure of 50 microns. Except for the bottom ½ in., the surfaces of the castings were good. This portion, as well as the top section of the casting containing the shrinkage head, was cropped. It was not necessary to overhaul the billets.

Hot Rolling. The desirable temperature range for rolling was specified as 595 to 650°C. In order to determine whether the temperature could be controlled within these limits, an experimental uranium billet 3 by 4 by 1½ in. thick was rolled. A chromel-alumel thermocouple was inserted into the billet so that temperature variations throughout the rolling and heating sequences could be followed. The billet was heated to 630°C in a mixture of 35% lithium carbonate–65% potassium carbonate and rolled on the two-high, standard, 6- by 10-in. mill with 10% reduction per pass. When the billet was finished at 0.200 in. in thickness, the recorder indicated that the thermocouple had failed on the last pass. It was ascertained from the data, however, that the heat generated during rolling was offset by the cooling effect of the rolls, and the over-all effect was simply that of arresting the cooling curve. It was concluded that the temperature of the billet never exceeded 650°C.

Two valuable sets of data were obtained from this experiment. Figure 26 shows the minimum reheat time required for uranium plate of varying thickness to again reach 630°C. Figure 27 shows the maximum permissible time between the salt bath and the rolls for uranium plate of varying thickness to be rolled at 600°C.

The twelve regular billets were hot rolled to the proper thickness from the salt bath, which was maintained at 630°C. Four of the 0.220-in.-thick plates were subsequently cold reduced 4%. A number of impressions, which were attributed to the lumps of salt, was noted on the plate surface. The other eight plates were sheared longitudinally and straightened in the tensile machine. The amount of plastic deformation required for straightening varied between 0.5 and 1.3%.

Samples will be cut from the plates for chemical, metallographic, and x-ray analysis and for thermal-cycling tests. Ultimately, dimensional stability of the material under irradiation will be investigated.

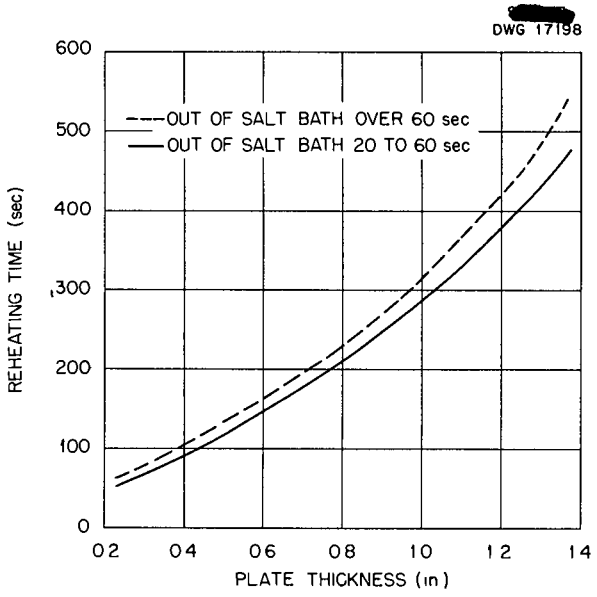

Fig. 26. Minimum Reheating Time Required for Uranium Plate of Varying Thickness to Reach 630°C in Salt Bath.

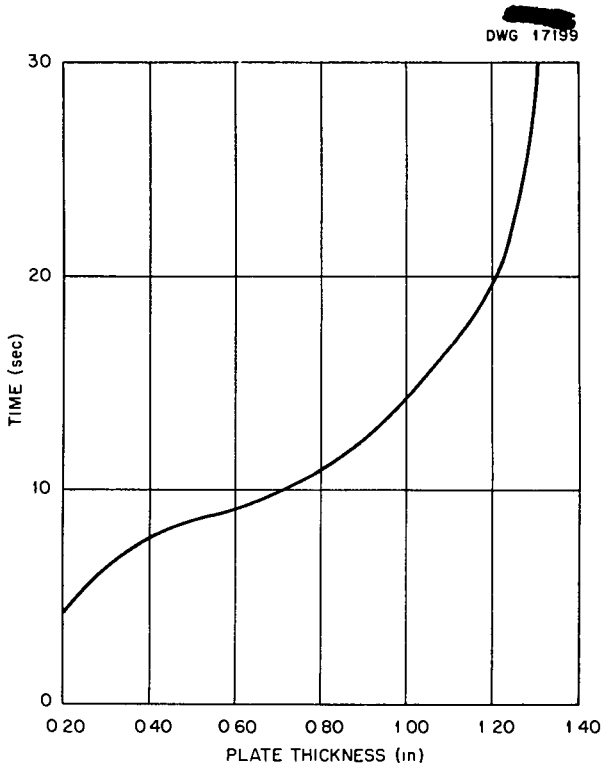

Fig. 27. Maximum Permissible Time Between Removal from Salt Bath and Rolling in Order to Roll Uranium Plate of Varying Thicknesses at 600°C.